



# HHS Public Access

Author manuscript

*J Immunol.* Author manuscript; available in PMC 2017 February 01.

Published in final edited form as:

*J Immunol.* 2016 February 1; 196(3): 1044–1059. doi:10.4049/jimmunol.1501962.

## iNKT-CELL ACTIVATION INDUCES LATE PRETERM BIRTH THAT IS ATTENUATED BY ROSIGLITAZONE<sup>1</sup>

Derek St Louis<sup>\*,†,‡,§,¶,ψ</sup>, Roberto Romero<sup>†,‡,§,¶,ψ</sup>, Olesya Plazyo<sup>\*,†,‡,§,¶,ψ</sup>, Marcia Arenas-Hernandez<sup>\*,†</sup>, Bogdan Panaitescu<sup>||</sup>, Yi Xu<sup>†</sup>, Tatjana Milovic<sup>\*</sup>, Zhonghui Xu<sup>\*,†</sup>, Gaurav Bhatti<sup>\*,†</sup>, Mi Qing-Sheng<sup>#,\*\*</sup>, Sascha Drewlo<sup>\*</sup>, Adi L. Tarca<sup>\*,†</sup>, Sonia S. Hassan<sup>\*,†</sup>, and Nardhy Gomez-Lopez<sup>\*,†,\*\*,2</sup>

<sup>\*</sup>Department of Obstetrics and Gynecology, Wayne State University School of Medicine, Detroit, Michigan, USA

<sup>†</sup>Perinatology Research Branch, Program for Perinatal Research and Obstetrics, Division of Intramural Research, *Eunice Kennedy Shriver* National Institute of Child Health and Human Development, NICHD/NIH/DHHS, Bethesda, Maryland, and Detroit, Michigan, USA

<sup>‡</sup>Department of Obstetrics and Gynecology, University of Michigan, Ann Arbor, Michigan, USA

<sup>§</sup>Department of Epidemiology and Biostatistics, Michigan State University, East Lansing, Michigan, USA

<sup>¶</sup>Center for Molecular Medicine and Genetics, Wayne State University, Detroit, Michigan, USA

<sup>||</sup>Department of Pediatrics, Neonatology Division, Wayne State University School of Medicine, Detroit, Michigan, USA

<sup>#</sup>Henry Ford Immunology Program, Henry Ford Health System, Detroit, Michigan, USA

<sup>\*\*</sup>Department of Immunology and Microbiology, Wayne State University School of Medicine, Detroit, Michigan, USA

### Abstract

Preterm birth (PTB) is a leading cause of neonatal morbidity and mortality; however, its non-infection-related mechanisms are poorly understood. Herein, we show that the expansion of activated CD1d-restricted invariant NKT (iNKT) cells in the third trimester by administration of  $\alpha$ -galactosylceramide ( $\alpha$ -GalCer) induces late PTB and neonatal mortality. *In vivo* imaging revealed that fetuses from mice that underwent  $\alpha$ -GalCer-induced late PTB had bradycardia and died shortly after delivery. Yet, administration of  $\alpha$ -GalCer in the second trimester did not cause pregnancy loss. PPAR $\gamma$  activation, through rosiglitazone treatment, reduced the rate of  $\alpha$ -GalCer-induced late PTB and improved neonatal survival. Administration of  $\alpha$ -GalCer in the third

<sup>1</sup>This research was supported by the Wayne State University Perinatal Initiative in Maternal, Perinatal and Child Health, and by the Perinatology Research Branch (PRB), Division of Intramural Research, *Eunice Kennedy Shriver* National Institute of Child Health and Human Development, National Institutes of Health, U. S. Department of Health and Human Services (NICHD/NIH/DHHS).

<sup>2</sup>Corresponding author: Nardhy Gomez-Lopez, PhD., Department of Obstetrics and Gynecology, Wayne State University School of Medicine, and the Perinatology Research Branch, NICHD/NIH/DHHS, Detroit, Michigan 48201, USA. Tel (313) 577-8904, Fax (313) 993 6769, nardhy.gomez-lopez@wayne.edu; ngomezlo@med.wayne.edu.

<sup>ψ</sup>The first three authors contributed equally to this work.

trimester suppressed PPAR $\gamma$  activation as shown by the down-regulation of *Fabp4* and *Fatp4* in myometrial and decidual tissues, respectively; this suppression was rescued by rosiglitazone treatment. Administration of  $\alpha$ -GalCer in the third trimester induced an increase in the activation of conventional CD4<sup>+</sup> T cells in myometrial tissues and the infiltration of activated macrophages, neutrophils and mature DCs to myometrial and/or decidual tissues. All of these effects were blunted after rosiglitazone treatment. Administration of  $\alpha$ -GalCer also up-regulated the expression of inflammatory genes at the maternal-fetal interface and systemically, and rosiglitazone treatment partially attenuated these responses. Finally, an increased infiltration of activated iNKT-like cells in human decidual tissues is associated with non-infection-related preterm labor/birth. Collectively, these results demonstrate that iNKT-cell activation *in vivo* leads to late PTB by initiating innate and adaptive immune responses and suggest that the PPAR $\gamma$  pathway has potential as a target for prevention of this syndrome.

## INTRODUCTION

Preterm birth (PTB) refers to the delivery of a live baby before the 37th week of gestation, and it is the leading cause of neonatal morbidity and mortality worldwide (1). In 2013, 11.39% of births in the United States were preterm (2). Preterm neonates are at an increased risk for short- and long-term morbidity, and prematurity represents a substantial burden for society (3–6). Approximately 72% (34 to <37 weeks) of all PTBs are diagnosed as late preterm (7, 8), and two thirds of all PTBs occur after spontaneous preterm labor (9). Therefore, we focused our attention on the elucidation of those mechanisms that lead to spontaneous late preterm labor/birth and the development of therapies to prevent this syndrome.

Inflammation is implicated in the pathological process of spontaneous preterm labor (10–38). Pathological inflammation can result from the activation of innate (39–47) immunity by microorganisms (24, 48) or endogenous danger signals derived from necrosis or cellular stress (44, 49–52) termed damage-associated molecular pattern molecules (53) or alarmins (54). The inflammatory process initiated by alarmins is known as sterile inflammation (55). The term ‘sterile intra-amniotic inflammation’ refers to an inflammatory process in which microorganisms cannot be detected in the amniotic cavity (44, 49–52, 56). Sterile intra-amniotic inflammation is more common than microbial-associated intra-amniotic inflammation in patients with spontaneous preterm labor (30, 57). Indeed, administration of alarmins such as IL1 $\alpha$  (58) or HMGB1 (59) induces preterm labor/birth. In addition, IL33, a classic alarmin (60), is expressed in decidual tissues and up-regulated in acute chorioamnionitis (61), a placental lesion associated with preterm labor (62). Recently, it was demonstrated that IL33 is a potent activator of invariant (i)NKT cells (63, 64). Therefore, we hypothesized that activation of iNKT cells, immune cells that can be activated by alarmins in the context of sterile inflammation, could participate in the immune mechanisms that lead to non-infection-related preterm labor/birth.

iNKT-cell activation induces the initiation of signaling pathways (e.g., the NF- $\kappa$ B pathway) that lead to the production of Th1 and Th2 cytokines and chemokines (65–70) which, in turn, leads to a massive immune response mediated by innate and adaptive immune cells

(71). Hence, we hypothesized that iNKT-cell activation via  $\alpha$ -galactosylceramide ( $\alpha$ -GalCer), a high affinity iNKT ligand (72, 73), would activate innate and adaptive immune cells at the maternal-fetal interface promoting pathological inflammation and leading to spontaneous preterm labor/birth. In addition, we proposed that suppression of this inflammatory response would prevent PTB induced by NKT-cell activation. In search of an anti-inflammatory drug to prevent PTB, we evaluated rosiglitazone, a selective peroxisome proliferator-activated receptor (PPAR) $\gamma$  agonist (74). Rosiglitazone causes activation of the PPAR $\gamma$  pathway which, in turn, suppresses gene transcription by interfering with signal transduction pathways, such as the NF- $\kappa$ B, STAT, and AP-1 pathways (75–77). PPAR $\gamma$  activation has been suggested as a therapeutic intervention for preventing PTB (78) since treatment with 15-deoxy-<sup>12,14</sup>-prostaglandin J<sub>2</sub> compound, a PPAR $\gamma$  agonist (79, 80), delays endotoxin-induced PTB (81). However, whether PPAR $\gamma$  activation blunts the inflammatory response induced by iNKT-cell activation has not been investigated.

Using a murine model, our investigations demonstrate for the first time that administration of  $\alpha$ -GalCer in the third trimester leads to late PTB, which is prevented following PPAR $\gamma$  activation by treatment with rosiglitazone. In addition, we describe that PPAR $\gamma$  activation regulates immune mechanisms locally, at the maternal-fetal interface, and systemically to attenuate  $\alpha$ -GalCer-induced late PTB. Finally, we broaden the significance of our findings by demonstrating an increase of activated iNKT-like cells in decidual tissue from women who underwent spontaneous preterm labor/birth.

## METHODS

### Animals

C57BL/6J (B6) mice were bred in the animal care facility at the C.S. Mott Center for Human Growth and Development at Wayne State University, Detroit, Michigan, USA, and housed under a circadian cycle (light: dark=12:12 h). Eight- to 12-week-old females were mated with male mice of proven fertility. Female mice were examined daily between 8:00 a.m. and 9:00 a.m. for the presence of a vaginal plug, which denoted 0.5 days *post-coitum* (dpc). Upon observation of vaginal plugs, female mice were then separated from the males and housed in other cages. The weight gain of two or more grams confirmed pregnancy at 12.5 dpc. Procedures were approved by the Institutional Animal Care and Use Committee (IACUC) at Wayne State University (Protocol No. A-09-08-12).

### $\alpha$ -GalCer-induced late preterm birth model

Pregnant B6 mice were i.v. injected with 1 $\mu$ g, 2 $\mu$ g, 3 $\mu$ g, or 4 $\mu$ g of  $\alpha$ -GalCer (KRN7000, Funakoshi Co., Ltd., Tokyo, Japan; n=3 each for 1 $\mu$ g, 3 $\mu$ g, or 4 $\mu$ g, and n=20 for 2 $\mu$ g) that had been dissolved in 50 $\mu$ l of 4% DMSO (Sigma-Aldrich Co., LLC, St. Louis, MO, USA) or with 50 $\mu$ l of 4% DMSO alone (referred to throughout the manuscript as DMSO) as a control (n=19) at 16.5 dpc (third trimester). Following injection, pregnant mice were monitored using a video camera with infrared light (Sony Corporation, China) until delivery. A second group of mice was i.v. injected with either 2 $\mu$ g of  $\alpha$ -GalCer or DMSO at 10.5 dpc (n=5 each; second trimester), and inspection of resorption sites was performed at 14.5 dpc. A third group of mice was i.v. injected with 2 $\mu$ g of  $\alpha$ -GalCer at 10.5 dpc (n=3) and monitored

during delivery; photographs of the neonates at 1 day and 2 days after birth were taken using a camera (Sony).

### **Video monitoring, pup mortality, and neonatal weight**

Video monitoring allowed for determination of gestational age and rate of pup mortality. Gestational age was calculated from the presence of the vaginal plug (0.5 dpc) until the observation of the first pup in the cage bedding. The rate of pup mortality for each litter was defined as the proportion of born pups found dead among the total litter size. Late PTB was defined as delivery between 18.0 and 18.5 dpc. Neonatal survival and weight were recorded after one week postpartum.

### ***In vivo* imaging by ultrasound**

On the morning of 16.5 dpc, pregnant B6 mice were anesthetized by inhalation of 2–3% isoflurane (Aerrane, Baxter Healthcare Corporation, Deerfield, IL, USA) and 1–2 L/min of oxygen in an induction chamber. Using Doppler ultrasound, the fetal heart rate and umbilical artery hemodynamic parameters were recorded (VisualSonics Inc., Toronto, ON, Canada). Following ultrasound, dams were placed under a heat lamp for recovery, which occurred 10–20 min after heating. On the same day at noon, dams were injected either with 2 $\mu$ g of  $\alpha$ -GalCer or DMSO as described previously (n=3 each). On the afternoon of 17.5 dpc (just prior to late PTB in those mice injected with  $\alpha$ -GalCer), a second ultrasound was performed, and the same hemodynamic parameters were evaluated.

### **Video monitoring by infrared thermography**

Pregnant B6 mice were i.v injected with 2 $\mu$ g of  $\alpha$ -GalCer at 16.5 dpc (n=3). Immediately after late preterm delivery, the body temperature of the newborns was monitored using a thermal infrared camera (FLIR e50, FLIR Systems, Inc., Wilsonville, OR, USA). Temperature readings were recorded at intervals of 15 and 30 sec, and also at intervals of 1, 2, 3.5, 5.5, and 8 min after birth. A newborn that maintained a constant body temperature was considered a viable pup, while a newborn that gradually decreased in body temperature to the level of room temperature was qualified as a dead pup; viable and dead pups were also confirmed by visual analysis.

### **Fetal and placental weights**

Pregnant B6 mice were i.v. injected with 2 $\mu$ g of  $\alpha$ -GalCer (n=8) or DMSO (n=6) at 16.5 dpc. Six hours after injection, dams were euthanized, and placental and fetal weights were recorded using a scale (DIA-20, American Weight Scales, Norcross, GA, USA).

### **Rosiglitazone treatment of $\alpha$ -GalCer-induced late PTB**

Pregnant B6 mice were i.v. injected with 2 $\mu$ g of  $\alpha$ -GalCer (n=14) at 16.5 dpc. After 2h, mice were s.c. injected with a 10 mg/kg of body weight dose of rosiglitazone (Selleck Chemicals, Houston, TX, USA) diluted in 1:10 DMSO. Control pregnant mice received only the dose of rosiglitazone at 16.5 dpc (n=10). Following injection, mice were monitored via video camera with infrared light until delivery (Figure 2A).

### Tissue collection from pregnant mice

Pregnant B6 mice were i.v. and/or s.c. injected at 16.5 dpc with: 1) DMSO, 2) 2 $\mu$ g of  $\alpha$ -GalCer, 3) 2 $\mu$ g of  $\alpha$ -GalCer followed by rosiglitazone (10 mg/kg of bodyweight) 2h after, or 4) rosiglitazone alone as a control. Mice were euthanized 6h after the injection with  $\alpha$ -GalCer or DMSO, or 4h after treatment with rosiglitazone (n=6–10 mice per group). Decidual and myometrial tissues from one implantation site were collected as previously described (82) and placed in RNAlater Stabilization Solution (Life Technologies, Grand Island, NY, USA) according to the manufacturer's instructions. Decidual and myometrial tissues from the remaining implantation sites were collected, and leukocytes were immediately isolated. The spleen, uterine lymph nodes (ULN), and liver were also collected, and leukocyte suspensions were prepared.

### Leukocyte isolation from murine tissues

Isolation of leukocytes from myometrial and decidual tissues was performed as previously described (82). Briefly, tissues were cut into small pieces using fine scissors and enzymatically digested with StemPro Cell Dissociation Reagent (Accutase, Life Technologies) for 35 min at 37°C. The spleen, ULN, and liver were gently dissociated using two glass slides in order to prepare a single leukocyte suspension. Leukocyte suspensions were filtered using a 100 $\mu$ m cell strainer (Fisher Scientific, Hanover Park, IL, USA), and washed with FACS buffer [0.1% bovine serum albumin (Sigma-Aldrich) and 0.05% sodium azide (Fisher Scientific Chemicals, Fair Lawn, NJ, USA) in 1X PBS (Fisher Scientific Bioreagents)] before immunophenotyping.

### Immunophenotyping of murine leukocytes

Leukocyte suspensions from decidual and myometrial tissues and the liver were stained using the LIVE/DEAD Fixable Blue Dead Cell Stain Kit (Life Technologies) prior to incubation with extracellular mAbs. Leukocyte suspensions were then centrifuged, and cell pellets were incubated for 10 min with the CD16/CD32 mAb (Fc $\gamma$ III/II Receptor; BD Biosciences, San Jose, CA, USA), and subsequently incubated with specific fluorochrome-conjugated anti-mouse mAbs (Supplementary Table I) for 30 min. Leukocyte suspensions were lysed/fixated with Lyse/Fix Buffer (BD Biosciences) for extracellular staining, and the BD Cytofix/Cytoperm™ Fixation/Permeabilization Solution Kit (BD Biosciences) for intracellular staining. At least 50,000 events for the spleen, liver, and decidual cells, or 25,000 events for the ULN and myometrial cells, were acquired using the BD LSRFortessa flow cytometer (BD Biosciences) and the FACSDiva 8.0 software (BD Biosciences). Leukocyte subsets were gated within the viability gate. Immunophenotyping included identification of: 1) CD1d-restricted iNKT cells (CD1d Tetramer+DX5+NK1.1+TCR $\beta$ + cells) and their activation status by expression of CD69, CD44, IFN $\gamma$ , and IL4; 2) conventional T cells (CD3+CD4+ and CD3+CD8+ cells) and their activation status by expression of CD69, CD25, PD1, CD40L, and CTLA-4; 3) neutrophils (CD11b+Ly6G+ cells) and their activation status by expression of IFN $\gamma$ ; 4) macrophages (CD11b+F4/80+ cells) and their activation status by expression of Arg1, iNOS, IFN $\gamma$ , and IL10; and 5) expression of IFN $\gamma$  by mature DCs (CD11b+CD11c+DEC205+ cells). Data were analyzed using the FACSDiva 8.0 software. The total number of specific leukocytes was determined

using CountBright absolute counting beads (Molecular Probes, Eugene, OR, USA). The figures were prepared using the FlowJo Software version 10 (FlowJo, LLC, Ashland, OR, USA).

### Gene expression determination

RNA was extracted from decidual and myometrial tissues using TRIzol Reagent (Life Technologies), QIAshredders (Qiagen, Valencia, CA, USA), RNase-Free DNase Sets (Qiagen), and RNeasy Mini Kits (Qiagen). RNA concentrations and purity were assessed with the NanoDrop 1000 spectrophotometer (Thermo Scientific, Wilmington, DE, USA), and RNA integrity was evaluated with the Bioanalyzer 2100 (Agilent Technologies, Wilmington, DE, USA). cDNA was synthesized using RT<sup>2</sup> First Strand Kits (Qiagen). The RT<sup>2</sup> Profiler Mouse PPAR Targets PCR Array (Qiagen) and RT<sup>2</sup> Profiler Mouse Inflammatory Cytokines & Receptors PCR Array (Qiagen) were used for initial screening (n=4 samples per group) and performed by using RT<sup>2</sup> SYBR Green ROX qPCR Mastermix (Qiagen) on a 7500 Fast Real-Time PCR System (Applied Biosystems, Life Technologies Corporation, Foster City, CA, USA). Expression profiling of those genes selected based on the screening results was confirmed by qRT-PCR using a BioMark High-throughput qRT-PCR System (Fluidigm, San Francisco, CA, USA) and an ABI 7500 FAST Real-Time PCR System (Applied Biosystems) using TaqMan gene expression assays (Applied Biosystems) (n=6–8 mice per group; Supplementary Table II).

### Chemokine/cytokine serum concentrations

Pregnant B6 mice were injected at 16.5 dpc with: 1) DMSO, 2) 2µg of α-GalCer, 3) 2µg of α-GalCer followed by rosiglitazone (10 mg/kg bodyweight) 2h after, or 4) rosiglitazone alone as a control. Mice were euthanized 6h or 24h after the injection with α-GalCer or DMSO (n=8–9 mice per group). Blood was recovered by cardiac puncture, and serum samples were separated by centrifugation and stored at -20°C until analysis. The Milliplex MAP Mouse Cytokine/Chemokine Kit (MCCYTOMAG-70K-PX32, EMD Millipore, Billerica, MA, USA) was used to measure the concentrations of G-CSF, GM-CSF, IFN $\gamma$ , IL1 $\alpha$ , IL1 $\beta$ , IL2, IL3, IL4, IL5, IL6, IL7, IL9, IL10, IL12p40, IL12p70, IL13, IL15, IL17, CCL11, CXCL10, CXCL1, LIF, CXCL5, CCL2, M-CSF, CXCL9, CCL3, CCL4, CXCL2, CCL5, and TNF- $\alpha$  in the serum samples according to the manufacturer's instructions. Plates were read using the Luminex 100 System (Luminex Corporation, Austin, TX, USA), and analyte concentrations were calculated using the xPONENT3.1 software (Luminex). The sensitivities of the assays were: 1.7pg/ml (G-CSF), 1.9pg/ml (GM-CSF), 1.1pg/ml (IFN $\gamma$ ), 10.3pg/ml (IL1 $\alpha$ ), 5.4pg/ml (IL1 $\beta$ ), 1.0pg/ml (IL2), 1.0pg/ml (IL3), 0.4pg/ml (IL4), 1.0pg/ml (IL5), 1.1pg/ml (IL6), 1.4pg/ml (IL7), 17.3pg/ml (IL9), 2.0pg/ml (IL10), 3.9pg/ml (IL12p40), 4.8pg/ml (IL12p70), 7.8pg/ml (IL13), 7.4pg/ml (IL15), 0.5pg/ml (IL17), 1.8pg/ml (CCL11), 0.8pg/ml (CXCL10), 2.3pg/ml (CXCL1), 1.0pg/ml (LIF), 22.1pg/ml (CXCL5), 6.7pg/ml (CCL2), 3.5pg/ml (M-CSF), 2.4pg/ml (CXCL9), 7.7pg/ml (CCL3), 11.9pg/ml (CCL4), 30.6pg/ml (CXCL2), 2.7pg/ml (CCL5), 2.3pg/ml (TNF- $\alpha$ ) and 0.3pg/ml (VEGF). Inter-assay and intra-assay coefficients of variation were below 15% and 4.9%, respectively.

## Human samples

Chorioamniotic membrane and basal plate samples were collected within 30 min after delivery from the Bank of Biological Specimens of the Perinatology Research Branch, an intramural program of the *Eunice Kennedy Shriver* National Institute of Child Health and Human Development, National Institutes of Health, U. S. Department of Health and Human Services (NICHD/NIH/DHHS), Wayne State University, and The Detroit Medical Center (Detroit, MI, USA). The Institutional Review Boards approved the collection and use of biological materials for research purposes. All participating women provided written informed consent. The study groups included women who delivered at term without labor (TNL), at term with labor (TIL), preterm without labor (PTNL), and preterm with labor (PTL). Demographic and clinical characteristics of these study groups are represented in Table I. Patients with multiple births or with neonates having congenital or chromosomal abnormalities were excluded. Labor was defined by the presence of regular uterine contractions at a frequency of at least two contractions every 10 minutes with cervical changes resulting in delivery (83). In each case, several tissue sections of the chorioamniotic membranes, umbilical cord, and placental disc were evaluated for acute chorioamnionitis and chronic chorioamnionitis, according to published criteria (84, 85), by pathologists who had been blinded to the clinical outcome.

## Decidual leukocyte isolation from human samples

Decidual leukocytes from human decidual tissue were isolated as previously described (86). Briefly, the decidua basalis was collected from the basal plate of the placenta, and the decidua parietalis was separated from the chorioamniotic membranes (Figure 8A). Decidual tissue was homogenized using a gentleMACS Dissociator (Miltenyi Biotec, San Diego, CA, USA) in StemPro Cell Dissociation Reagent. Homogenized tissues were incubated for 45 min at 37°C with gentle agitation. After incubation, tissues were washed in ice-cold 1X PBS (Life Technologies) and filtered through a 100µm cell strainer. Cell suspensions were collected and centrifuged at 300 x g for 10 min, and the cell pellet was suspended in FACS buffer. Mononuclear leukocytes were purified using a density gradient (Ficoll-Paque Plus; GE Healthcare Bio-Sciences AB, Sweden), following the manufacturer's instructions. Lastly, mononuclear cell suspensions were washed using FACS buffer before immunophenotyping.

## Immunophenotyping of human decidual leukocytes

Mononuclear cell suspensions from decidual tissues were stained with BD Horizon Fixable Viability Stain 510 dye (BD Biosciences) prior to incubation with extracellular mAbs. Mononuclear cell suspensions were then washed with staining buffer (Cat No. 554656; BD Biosciences) and centrifuged. Cell pellets were incubated for 10 min with FcR Blocking Reagent (Cat No. 130-059-901; Miltenyi Biotec). Next, mononuclear cell suspensions were incubated with the following fluorochrome-conjugated anti-human mAbs: CD14-BUV395 (clone MφP9; BD Biosciences), CD15-BV605 (clone W6D3; BD Biosciences), CD3-BV650 (clone OKT3; BD Biosciences), CD19-BUV737 (clone SJ25C1; BD Biosciences), CD56-PE-Cy7 (clone NCAM16.2; BD Biosciences), CD69-Alexa Fluor 700 (clone FN50; BD Biosciences) and Vα24Ja18TCR-PE (clone 6B11; eBioscience; San Diego, CA, USA)

for 30 min at 4 °C in the dark. Finally, mononuclear cell suspensions were washed and re-suspended in 0.5ml of staining buffer and acquired using the BD LSRFortessa flow cytometer and FACSDiva 6.0 software. Leukocyte subsets were gated within the viability gate, and activated iNKT-like cells were identified as CD15–CD14–CD19–CD3+CD56+CD69+ or CD3+V $\alpha$ 24J $\alpha$ 18TCR+CD69+ cells. The analysis was performed, and the figures generated using FlowJo Software version 10.

### Immunofluorescence

Immediately after collection, the chorioamniotic membranes were frozen in Tissue-Plus O.C.T. Compound (Fisher HealthCare, Houston, TX, USA). Ten- $\mu$ m-thick cryosections were cut, placed on Fisherbrand Superfrost Plus microscope slides (Thermo Scientific, Waltham, MA, USA), fixed with 4% paraformaldehyde (Electron Microscopy Sciences, Hatfield, PA, USA), and washed with 1X PBS. Non-specific antibody interaction was blocked using a Protein Blocker serum-free (Cat No. X0909; Dako North America, Carpinteria, CA, USA) for 30 min at room temperature. Slides were then incubated with the following anti-human mAbs: mouse CD69-FITC (LifeSpan BioSciences, Inc., Seattle, WA, USA), mouse CD56-APC (clone MEM-188, BioLegend, San Diego, CA, USA), and rabbit CD3 (Abcam, Cambridge, MA, USA) at 4°C overnight. Following incubation, slides were washed with 1X PBS containing 0.1% Tween-20 (Sigma-Aldrich). Secondary goat anti-rabbit IgG-Alexa Fluor 594 (Invitrogen, Molecular Probes, Eugene, OR, USA) was added for CD3 detection, and slides were incubated for 1h at room temperature. Slides were washed and mounted with the ProLong Gold Antifade reagent with DAPI (Life Technologies). Immunofluorescence was visualized using a Zeiss LSM 780 laser scanning confocal microscope (Carl Zeiss Microscopy GmbH, Jena, Germany) at the Microscopy, Imaging and Cytometry Resources Core at Wayne State University School of Medicine (<http://micr.med.wayne.edu/>). Immunofluorescence signals for APC, Alexa Fluor 594, and FITC were excited using a 633 nm HeNe laser, a 561 nm HeNe laser, and the 488 nm line of a Multiline Argon laser, respectively. The DAPI signal was excited using a 405 nm diode laser.

### Statistical analysis

Observational mouse data were analyzed using IBM SPSS, version 19.0, and all other analyses were performed in R (<http://www.R-project.org/>). For the gestational age, rate of pup mortality, and ultrasound parameters, the statistical significance of group comparisons was assessed using Mann-Whitney U tests. For flow cytometry data, the statistical significance of group comparisons was assessed using Mann-Whitney U tests. For fetal, placental, and neonatal weights, the statistical significance of group comparisons was assessed using pooled variance t-tests after log transformation. For qRT-PCR arrays, negative Ct values determined using multiple reference genes (*Gusb*, *Hsp90ab1*, *Gapdh* and *Actb*) averaged within each sample to determine gene expression levels. A heat map was created for the group mean expression matrix (gene x group mean) with each gene expression level being first standardized. A hierarchical clustering tree of genes was constructed using 1-Pearson correlation as distance metric and average linkage, while treatment groups clustering was based on an Euclidean distance with Ward linkage. For Fluidigm qPCR assays, negative Ct values were calculated using *Actb* as a reference gene.



For Fluidigm gene expression and cytokine concentrations, statistical tests of group differences were performed using linear models, and whenever data was left, right, or interval censored, a survival regression model with Gaussian error was used instead. Human demographic data were analyzed using IBM SPSS, version 19, and comparisons among the groups were performed using Chi-square tests for proportions as well as Kruskal-Wallis tests for non-normally distributed continuous variables. For proportions of activated iNKT-like cells in human decidual tissues, statistical significance of group differences was assessed using Mann-Whitney U tests. A p-value of  $< 0.05$  was used to determine statistical significance.

## RESULTS

### $\alpha$ -GalCer administration in the third trimester induces late preterm birth

Intravenous administration of 2 $\mu$ g of  $\alpha$ -GalCer during the third trimester caused 75 $\pm$ 18.9% of births to be categorized as late preterm (birth occurring between 18.0 and 18.5 dpc;  $\alpha$ -GalCer-induced late PTB), while DMSO (control) resulted in no late PTB (Figure 1A). Consequently, dams that were i.v. injected with 2 $\mu$ g of  $\alpha$ -GalCer had shorter gestations than the DMSO control group (Figure 1B). A high proportion of preterm pups were found dead minutes after delivery (Figure 1C). Intravenous administration of 3 $\mu$ g or 4 $\mu$ g of  $\alpha$ -GalCer induced very early PTB (birth occurring before 17.5 dpc with 100% pup mortality); however, 1 $\mu$ g of  $\alpha$ -GalCer did not cause PTB (data not shown). These data demonstrate that  $\alpha$ -GalCer administration in the third trimester induces late PTB and pup mortality.

### $\alpha$ -GalCer administration in the third trimester causes neonatal death

Dams that were injected with  $\alpha$ -GalCer delivered premature viable and non-viable pups. We then investigated whether these pups were dying in the uterus (fetal death) or after delivery (neonatal death). Abnormal umbilical artery velocimetry and fetal heart rate are associated with fetal compromise (87–90). Therefore, Doppler ultrasound was performed on 17.5 dpc, just prior to late PTB in those mice injected with  $\alpha$ -GalCer. The umbilical artery pulsatility index did not differ between fetuses from dams injected with  $\alpha$ -GalCer and DMSO (Figure 1D). However, bradycardia, a reduction of the heart rate, occurred in fetuses from dams injected with  $\alpha$ -GalCer when compared to the DMSO control (Figure 1E). These data demonstrated that, although pups do not die in the uterus, their health was compromised before birth. Administration of  $\alpha$ -GalCer also reduced fetal and placental weights, but did not decrease the weight of one-week-old neonates (Supplementary Figure 1A–C). To further evaluate when the premature pups died, we placed dams injected with  $\alpha$ -GalCer under video surveillance using infrared thermography. A high proportion of premature pups died within 10 min of delivery. In Figure 1F, representative frames demonstrate that the body temperature of a non-viable premature pup (red circle) reduced quickly from 30.5°C to 21.3°C. Conversely, a viable premature pup kept a constant temperature of 23.3°C to 23.1°C (green circle).

### $\alpha$ -GalCer administration in the second trimester does not cause pregnancy loss

During mid-pregnancy, iNKT-cell activation by i.p. administration of  $\alpha$ -GalCer (100 $\mu$ g/kg of body weight, ~2.5 $\mu$ g) leads to pregnancy loss (91, 92). Herein, we demonstrated that i.v.

administration of 2 $\mu$ g of  $\alpha$ -GalCer in the second trimester did not cause pregnancy loss (Figure 1G). However, we could not rule out the possibility that this dose would cause PTB or have deleterious effects on neonates. Therefore, neonates from dams injected with  $\alpha$ -GalCer at 10.5 dpc were observed up to one week post-partum. All delivered pups were viable and appeared healthy. Figure 1H shows viable term pups at 1 day and 2 days post-partum from dams injected with  $\alpha$ -GalCer in the second trimester.

### Rosiglitazone treatment reduces the rate of $\alpha$ -GalCer-induced late preterm birth

iNKT-cell activation can initiate the NF- $\kappa$ B pathway, leading to production of Th1 cytokines, such as IFN $\gamma$  (67). We then hypothesized that activation of the PPAR $\gamma$  pathway by administration of rosiglitazone, which interferes with the NF- $\kappa$ B pathway (75, 76), would prevent  $\alpha$ -GalCer-induced late PTB. Dams that were injected with  $\alpha$ -GalCer and subsequently treated with rosiglitazone had a 40% reduction in the rate of late PTB in comparison to dams injected with  $\alpha$ -GalCer alone (35.7 $\pm$ 25.1% vs. 75 $\pm$ 18.9%; Figure 2B). Consequently, gestational age was greater in dams treated with rosiglitazone after  $\alpha$ -GalCer injection than in dams injected with  $\alpha$ -GalCer alone (Figure 2C). Importantly, dams that were treated with rosiglitazone after an injection of  $\alpha$ -GalCer had a 30% reduction in pup mortality when compared to dams injected with  $\alpha$ -GalCer alone (Figure 2D). These results demonstrate that treatment with rosiglitazone can prevent  $\alpha$ -GalCer-induced late PTB and improve neonatal outcomes.

### $\alpha$ -GalCer inhibits PPAR $\gamma$ activation at the maternal-fetal interface that is restored by rosiglitazone

Since treatment with rosiglitazone reduced the rate of  $\alpha$ -GalCer-induced late PTB, we investigated whether  $\alpha$ -GalCer was inhibiting PPAR $\gamma$  genes at the maternal-fetal interface and whether this inhibition could be abrogated by rosiglitazone. Expression profiles of the PPAR pathway-related genes were different between myometrial and decidual tissues in all of the groups (Figure 2E). We specifically focused on PPAR $\gamma$  target genes. Adipocyte-specific fatty acid binding protein (*Fabp4*) and fatty acid transport protein 4 (*Fatp4*) are recognized as indicators of PPAR $\gamma$  activation (93, 94). Our array data showed that rosiglitazone up-regulated *Fabp4* in myometrial tissues and *Fatp4* and *Cyp410* in decidual tissues while  $\alpha$ -GalCer down-regulated such genes; therefore, we validated the expression of *Fabp4* and *Fatp4* in these tissues. Administration of  $\alpha$ -GalCer down-regulated expression of *Fabp4* in myometrial tissues; however, treatment with rosiglitazone resulted in up-regulation to basal levels (Figure 2F). Administration of  $\alpha$ -GalCer down-regulated expression of *Fatp4* in myometrial tissues and tended to down-regulate expression of *Fatp4* in decidual tissues (Figure 2G). Treatment with rosiglitazone partially restored *Fatp4* expression in decidual tissues but not in myometrial tissues (Figure 2G). These results demonstrate that rosiglitazone prevents  $\alpha$ -GalCer-induced late PTB by restoring PPAR $\gamma$  activation at the maternal-fetal interface.

### **$\alpha$ -GalCer induces an expansion of activated CD1d-restricted iNKT cells in decidual tissues that is blunted by rosiglitazone**

Next, we investigated whether  $\alpha$ -GalCer caused a systemic and local (maternal-fetal interface) expansion of iNKT cells and whether rosiglitazone reduced such expansions. Because NKT-cell function and subsets are tissue- or organ-specific (95–97), we used a combination of markers including CD1d-Tetramer loaded with  $\alpha$ -GalCer, DX5, NK1.1, and TCR $\beta$  to identify iNKT cells (Figure 3A). Administration of  $\alpha$ -GalCer caused an expansion of CD1d-restricted iNKT cells (CD1d Tetramer+DX5+TCR $\beta$ +NK1.1+ cells) in decidual tissues; yet, this expansion was blunted by treatment with rosiglitazone (Figures 3B). In contrast, administration of  $\alpha$ -GalCer did not significantly alter the number of CD1d-restricted iNKT cells in the liver (Supplementary Figure 2A), myometrium (Supplementary Figure 2B), spleen (Supplementary Figure 2C), or ULN (Supplementary Figure 2D).

We also evaluated whether  $\alpha$ -GalCer-expanded decidual iNKT cells were activated and, in such a case, whether rosiglitazone treatment reduced the number of these cells. Activated iNKT cells express CD69 and CD44, and release Th1 (e.g., IFN $\gamma$ ) and Th2 cytokines (e.g., IL4) (67, 69, 98). Decidual CD1d-restricted iNKT cells expressed CD69, CD44, IL4 (Figure 3C), and, to a lesser extent, IFN $\gamma$  (Supplementary Figure 3). Administration of  $\alpha$ -GalCer increased the number of activated CD69+CD44+ and IL4+CD1d-restricted iNKT cells in decidual tissues, both of which were reduced by treatment with rosiglitazone (Figure 3D&E). No significant effects were seen in IFN $\gamma$ +CD1d-restricted iNKT cells upon  $\alpha$ -GalCer and/or rosiglitazone administration (Supplementary Figure 3). Together, these data demonstrate that rosiglitazone prevents  $\alpha$ -GalCer-induced late PTB by reducing activated CD1d-restricted iNKT cells at the maternal-fetal interface.

### **$\alpha$ -GalCer induces activation of conventional CD4+ T cells in myometrial tissues that is reduced by rosiglitazone**

iNKT cells bridge the innate and adaptive limbs of the immune system; therefore, activation of iNKT cells triggers both innate and adaptive immune responses (99). Indeed, activation of CD1d-restricted iNKT cells by administration of  $\alpha$ -GalCer in non-pregnant mice induces expression of CD69, an early activation marker, in T cells and B cells (100–103). We then investigated whether administration of  $\alpha$ -GalCer in the third trimester induced T-cell activation in myometrial and decidual tissues, and whether this activation was reduced after treatment with rosiglitazone. Several markers of T-cell activation including CD25, CD40L, PD1, CD69, and CTLA-4 were determined in conventional CD4+ and CD8+ T cells. Administration of  $\alpha$ -GalCer led to the activation of conventional CD4+ T cells demonstrated by the expression of CD25 and PD1 in myometrial tissues, which was reduced by treatment with rosiglitazone (Figures 4A–C). This treatment also reduced basal CD8+ T cell activation in myometrial tissues (Figures 4D&E). No significant effects were seen in activated CD4+ and CD8+ T cells upon  $\alpha$ -GalCer administration in decidual tissues (Supplementary Figure 4). These data demonstrate that rosiglitazone prevents  $\alpha$ -GalCer-induced late PTB by reducing activated T cells in the myometrial tissues.

### **$\alpha$ -GalCer induces innate immune activation at the maternal-fetal interface that is attenuated by rosiglitazone**

iNKT-cell activation also initiates innate immune responses mediated by macrophages and neutrophils (102, 104) as well as induces the full maturation of DCs manifested by the expression of MHC class II, IFN $\gamma$  production, and APC function (105).

First, we investigated whether administration of  $\alpha$ -GalCer induces macrophage activation in myometrial and decidual tissues, and whether this activation was reduced after treatment with rosiglitazone. Macrophage activation is a complex process since it depends on the nature of the stimulus and the microenvironment where these cells exhibit their function (106, 107). The classical M1/M2 macrophage paradigm provides useful markers (Arg1, iNOS, IL10, and IFN $\gamma$ ) for macrophage activation (108–111); therefore, we evaluated the expression of these molecules in myometrial and decidual macrophages (CD11b+F4/80+ cells). Administration of  $\alpha$ -GalCer increased the number of decidual macrophages that produce both IFN $\gamma$  and IL10 (Figure 5A). Also, administration of  $\alpha$ -GalCer increased the number of decidual macrophages that express both Arg1 and IL10; yet, this increase did not reach statistical significance (Figure 5B). In both cases, treatment with rosiglitazone reduced the number of activated macrophages (Figures 5A&B). Administration of  $\alpha$ -GalCer did not have such effects on myometrial macrophages (data not shown).

Next, we investigated whether administration of  $\alpha$ -GalCer induces neutrophil activation in myometrial and decidual tissues, and whether this activation was reduced after treatment with rosiglitazone. IFN $\gamma$  expression is an indicator of neutrophil activation (112, 113). In the study herein, we demonstrated that administration of  $\alpha$ -GalCer increased the expression of IFN $\gamma$  by neutrophils in myometrial and decidual tissues, and this effect was reduced by treatment with rosiglitazone (Figures 5C & Supplementary Figure 5).

Lastly, we investigated whether administration of  $\alpha$ -GalCer in the third trimester induced DC maturation in decidual tissues, and whether this process was blocked by administration of rosiglitazone. Administration of  $\alpha$ -GalCer increased the number of mature DCs (CD11b+CD11c+DEC205+ cells; data not shown) and the number of IFN $\gamma$ + mature DCs in decidual tissues (Figure 5D). Treatment with rosiglitazone did not reduce the number of mature DCs (data not shown); however, it reduced the number of IFN $\gamma$ + mature DCs in decidual tissues (Figure 5D).

Taken together, these data demonstrate that rosiglitazone prevents  $\alpha$ -GalCer-induced late PTB by attenuating innate immune activation at the maternal-fetal interface.

### **$\alpha$ -GalCer induces a pro-inflammatory microenvironment at the maternal-fetal interface that is partially attenuated by rosiglitazone**

Whereas iNKT-cell activation induces the expression of inflammatory genes (65, 66), PPAR $\gamma$  activation suppresses their expression (75, 76). We next investigated whether  $\alpha$ -GalCer up-regulated inflammatory genes at the maternal-fetal interface, and whether this up-regulation was suppressed by rosiglitazone. Expression profiles of inflammation-related genes were different between decidual and myometrial tissues (Figure 6A). As expected, several genes were up-regulated in both types of tissue upon administration of  $\alpha$ -GalCer ( $\alpha$ -

GalCer vs. DMSO; Figure 6A). Some of these genes were down-regulated after treatment with rosiglitazone, mainly in decidual tissues ( $\alpha$ -GalCer+Rosi vs.  $\alpha$ -GalCer; Figure 6A). We selected some of the down-regulated genes after treatment with rosiglitazone and validated their expression. Administration of  $\alpha$ -GalCer up-regulated the expression of *Ccl1*, *Ccl2*, *Ccl12*, and *Tnf* in decidual tissues; however, these genes were down-regulated after treatment with rosiglitazone (Figure 6B). Administration of  $\alpha$ -GalCer also up-regulated expression of *Ccl2* and *Ccl12* in myometrial tissues; however, only *Ccl2* was significantly down-regulated after treatment with rosiglitazone (Figure 6C). These data demonstrate that rosiglitazone prevents  $\alpha$ -GalCer-induced late PTB by partially reducing the pro-inflammatory milieu at the maternal-fetal interface.

### **$\alpha$ -GalCer induces a maternal systemic pro-inflammatory response, yet rosiglitazone triggers a maternal systemic anti-inflammatory response**

Next, we evaluated the effects of  $\alpha$ -GalCer and rosiglitazone on cytokine serum concentration in maternal circulation at 6h or 24h (prior to  $\alpha$ -GalCer-induced late PTB) post  $\alpha$ -GalCer administration. Six hours post  $\alpha$ -GalCer administration, the concentrations of all measured cytokines, except GMSCF, IL3, IL4, and IL7, were increased when compared to DMSO or rosiglitazone controls; however, none of these cytokines were reduced after treatment with rosiglitazone (data not shown). Twenty-four hours post  $\alpha$ -GalCer administration, the pro-inflammatory cytokines —IFN $\gamma$ , IL2, CXCL9, CXCL10, CCL2, and CCL5 — were increased when compared to DMSO or rosiglitazone controls (Figure 7A). Treatment with rosiglitazone did not reduce these high concentrations; indeed, it further increased the concentrations of IFN $\gamma$ , CXCL9, CXCL10, and CCL2 (Figure 7A). Interestingly, dams injected with  $\alpha$ -GalCer that were subsequently treated with rosiglitazone had increased concentrations of anti-inflammatory cytokines IL10, IL17, IL3, IL5, GSCF, and IL12p40 when compared to mice injected with only  $\alpha$ -GalCer (Figure 7B). These data demonstrate that rosiglitazone prevents  $\alpha$ -GalCer-induced late PTB by enhancing a maternal systemic anti-inflammatory response.

### **Spontaneous preterm labor/birth is associated with an increased proportion of activated iNKT-like cells in decidual tissues**

Up to this point, our results demonstrated that activation of decidual iNKT cells leads to late PTB in mice; however, it was unknown whether these cells are increased during preterm labor/birth in humans. iNKT cells are present in first-trimester decidua (114); therefore, we hypothesized that preterm labor will be associated with an increase in the proportion of activated iNKT cells at the maternal-fetal interface. In humans, the maternal-fetal interface includes: 1) the decidua parietalis that lines the uterine cavity not covered by the placenta and is in juxtaposition to the chorion leave, and 2) the decidua basalis, located in the basal plate of the placenta where it is invaded by interstitial trophoblasts (Figure 8A). The gating strategy used to determine activated iNKT-like cells

(CD69+CD56+CD3+CD19-CD14-CD15- cells) in decidual tissues is shown in Figure 8B. In the decidua basalis and parietalis, activated iNKT-like cells were greater in women who underwent spontaneous term labor (TIL) or preterm labor (PTL) when compared to women who did not undergo labor at term (TNL) or preterm (PTNL), respectively (Figure 8C). In the decidua basalis, activated iNKT-like cells were more abundant in PTL samples than in

TIL samples (Figure 8C). Further immunophenotyping of decidual samples (TIL and PTL, n=4 each) revealed that activated iNKT cells (CD3+V $\alpha$ 24J $\alpha$ 18TCR+CD69+ cells; Figure 8D) were present at proportions similar to previously identified activated iNKT-like cells (CD3+CD56+CD69+ cells) (Figure 8B). Since we did not use the iNKT marker, V $\alpha$ 24J $\alpha$ 18TCR, in our initial immunophenotyping, we cannot refer to these as iNKT cells and have instead termed them iNKT-like cells. Localization of activated iNKT-like cells (CD3+CD56+CD69+DAPI+ cells; white arrows) in the decidua parietalis is shown in Figure 8E. This last set of data demonstrates that activated iNKT-like cells in human decidual tissues are linked to spontaneous preterm labor/birth.

## DISCUSSION

Sterile intra-amniotic inflammation is more frequent than microbial-associated intra-amniotic inflammation in patients with spontaneous preterm labor (30, 57). Sterile inflammation is initiated by alarmins (55) and such danger signals are potent activators of iNKT cells (63, 64); therefore, we hypothesized that these innate lymphocytes participate in the pathophysiology of sterile inflammation-related preterm labor/birth. Using a highly-affine iNKT-cell ligand,  $\alpha$ -GalCer (73), we provided direct evidence that iNKT-cell activation is implicated in the mechanisms that lead to inflammation-induced preterm labor in the absence of infection. Indirect evidence for the role of iNKT cells in the pathophysiology of inflammation-induced preterm labor was based on two facts: (1) iNKT-cell null mice (*Ja18*<sup>-/-</sup> mice) are more resistant to endotoxin-induced PTB than wild type mice (115), and (2) adoptive transfer of decidual iNKT cells into iNKT-cell null mice injected with an endotoxin rapidly induces the onset of PTB (116). However, endotoxins are not iNKT-cell ligands and can only indirectly activate autoreactive iNKT cells through TLR signaling and the release of IL12 by APCs (68, 71, 117). Therefore, indirect activation of iNKT cells by an endotoxin resembles Gram-negative bacteria-related preterm labor, and direct activation via an iNKT-cell ligand could explain sterile inflammation-related preterm labor.

Administration of  $\alpha$ -GalCer in the second trimester did not result in pregnancy loss. This finding is not surprising since the mechanisms that lead to pregnancy loss differ from those implicated in preterm labor/birth. For example, during the second trimester, pregnancy maintenance depends on regulatory T cells (Tregs), as their depletion causes pregnancy loss (118, 119). In the third trimester, however, depletion of Tregs does not cause preterm labor/birth (120). These data led us to suggest that during the third trimester, Treg-independent regulatory mechanisms such as iNKT-cell quiescence may be responsible for pregnancy maintenance. Further studies are needed to investigate the mechanisms whereby iNKT cells remain quiescent in order to maintain pregnancy until term.

Late preterm neonates survive, yet are at a higher risk for morbidity and mortality than term neonates (121, 122). In our model of  $\alpha$ -GalCer-induced late PTB, we consistently showed that pups did not die *in utero*; yet, they were bradycardic and died shortly after birth. This finding indicated that fetal compromise was occurring simultaneously with the process of preterm labor rather than as a direct cause of prematurity. Because NKT cells appear at day 5 after birth (123), we are confident that the adverse neonatal outcomes are due to the effects

of  $\alpha$ -GalCer administration on the maternal immune system and at the maternal-fetal interface rather than as a direct effect on the pups.

Herein, we demonstrated for the first time that  $\alpha$ -GalCer inhibits PPAR $\gamma$  activation at the maternal-fetal interface, which is concordant with a previous study demonstrating that PPAR $\gamma$  expression is reduced in intrauterine tissues in term parturition (124). These data suggest that PPAR $\gamma$  activation, a suppression of inflammatory genes, is required for late pregnancy maintenance and its inhibition participates in the normal and pathological processes of labor. Conversely, rosiglitazone causes PPAR $\gamma$  activation and prevents  $\alpha$ -GalCer-induced late PTB. Our unpublished results demonstrated that this PPAR $\gamma$  agonist also prevents endotoxin-induced PTB (125). Therefore, targeting the PPAR $\gamma$  pathway could represent a new strategy to prevent both sterile and microbial inflammation-related preterm labor/birth.

An expansion of decidual iNKT cells was observed shortly after  $\alpha$ -GalCer administration. This is consistent with a previous study demonstrating that iNKT-cell activation is observed only 4 hours post- $\alpha$ -GalCer administration (92). A systemic expansion of iNKT cells occurs 2–3 days after  $\alpha$ -GalCer administration (126), which explains why in our study we did not observe such an event. We also demonstrated that treatment with rosiglitazone attenuated the  $\alpha$ -GalCer-induced iNKT-cell expansion in decidual tissues. It is likely that rosiglitazone is interfering with iNKT-cell development instead of causing cell death, since this drug did not reduce cell viability in decidual cells (Supplementary Figure 6); yet, it caused a reduction of iNKT cells in the liver (Supplementary Figure 2A). The previous hypothesis is supported by the fact that PPAR $\gamma$  activation regulates CD1d molecules (93, 127), which are constitutively expressed by APCs (128, 129) and can modulate iNKT-cell responses (71, 130). Therefore, it is probable that indirect suppression of iNKT-cell expansion and activation is the primary mechanism whereby rosiglitazone prevents PTB in our model. Consequently, we investigated whether rosiglitazone could be suppressing activation/maturation of T cells, macrophages, neutrophils, and DCs, all of which are implicated in the pathophysiology of preterm labor/birth (47, 131, 132).

T cells seem to be implicated in the process of preterm parturition (132). This concept was based on the fact that mice deficient in T and B cells (*Rag1*<sup>-/-</sup>) are more susceptible to endotoxin-induced PTB than wild type mice, and this susceptibility is reversed upon transfer of CD4<sup>+</sup> T cells (133). These findings led us to suggest that CD4<sup>+</sup> T cells play a regulatory role in late pregnancy (132); however, their function has not been established by depleting these cells prior to preterm labor. Recently, we proposed that the activation of effector CD4<sup>+</sup> T cells is involved in the physiological process of parturition (134–136). Herein, we provide further evidence to this hypothesis by demonstrating that activation of CD4<sup>+</sup> T cells occurs prior to  $\alpha$ -GalCer-induced PTB. We also demonstrated that rosiglitazone reduced  $\alpha$ -GalCer-induced T-cell activation. This finding is consistent with previous studies demonstrating that pretreatment with PPAR $\gamma$  ligands reduces T-cell activation and proliferation *in vitro* (137, 138). Taken together, these data support the hypothesis that CD4<sup>+</sup> T cell activation participates in the physiological and pathological processes of parturition and suggests that targeting the PPAR $\gamma$  pathway attenuates activation of the adaptive limb of immunity, rescuing preterm labor/birth.

The role of macrophages in the mechanisms that lead to preterm labor is well-established since the depletion of these innate cells protects mice from endotoxin-induced PTB (139). The study herein demonstrated increased macrophage activation prior to  $\alpha$ GalCer-induced PTB, which supports a central role for these innate immune cells in the pro-inflammatory milieu that accompanies the sterile processes of preterm parturition. We also demonstrated that treatment with rosiglitazone inhibits macrophage activation in decidual tissues. Prior research, in line with our study, has shown that PPAR $\gamma$  expression is up-regulated in activated macrophages and that treatment with rosiglitazone, or natural PPAR $\gamma$  agonists, down-regulates the expression of iNOS, inhibits migration, and suppresses the release of inflammatory cytokines by these cells (75, 140, 141).

Unlike macrophages, the depletion of neutrophils does not prevent endotoxin-induced PTB; yet, it ameliorates the pro-inflammatory response in the uterine-placental tissues (142). Herein, we demonstrated that activation of neutrophils occurs prior to  $\alpha$ GalCer-induced preterm birth, which suggests that although neutrophils are not essential, they participate in the pro-inflammatory milieu that accompanies the pathological process of preterm parturition. We also found that treatment with rosiglitazone reduced  $\alpha$ -GalCer-induced neutrophil activation. This is in accord with a previous *in vitro* study which demonstrated that PPAR $\gamma$  agonists (troglitazone and 15-deoxy-<sup>12,14</sup> prostaglandin J<sub>2</sub>) diminished the chemotactic response of neutrophils and suppressed their production of pro-inflammatory cytokines (143).

In addition, administration of  $\alpha$ -GalCer resulted in the expression of IFN $\gamma$  by mature decidual DCs. These innate immune cells seem to contribute to the initiation of T cell responses during the physiological and pathological processes of parturition (132, 133, 136, 144, 145). Herein, we provide evidence to support this hypothesis by demonstrating that mature DCs participate in the inflammatory process that leads to inflammation-related preterm labor/birth. We also showed that treatment with rosiglitazone blunted the  $\alpha$ -Galcer-induced IFN $\gamma$  expression in mature DCs but did not interfere in their maturation. This is consistent with a previous study demonstrating that rosiglitazone does not interfere with the maturation of DCs *in vitro* nor affects their ability to activate T cells *in vivo*; however, this PPAR $\gamma$  agonist modifies DC differentiation by reducing their secretion of cytokines (146).

Collectively, our results demonstrated that prior to  $\alpha$ -Galcer-induced PTB there was an activation of innate immune cells at the maternal-fetal interface, which were suppressed by PPAR $\gamma$  activation, rescuing inflammation-related preterm labor/birth.

Besides regulating immune cell activation at the maternal-fetal interface, rosiglitazone attenuated the expression of pro-inflammatory cytokine/chemokines implicated in the pathophysiology of inflammation-related preterm labor (147–155). The suppressive effect of PPAR $\gamma$  agonists on cytokine expression has been previously demonstrated *in vitro* (156). These data demonstrate that PPAR $\gamma$  activation regulates the local pro-inflammatory milieu associated with preterm labor/birth.

The systemic anti-inflammatory activity of rosiglitazone was also demonstrated in this study. This finding is in concordance with our unpublished data showing that treatment with



rosiglitazone increases the serum concentration of IL5 and CXCL9 in dams injected with an endotoxin (Yi Xu, et al; unpublished data). The immunomodulatory action of rosiglitazone through the up-regulation of anti-inflammatory cytokines was previously demonstrated when PMA-stimulated THP-1 cells were incubated with PPAR $\gamma$  agonists and an increased production of IL1RA was observed (157). In our study, the anti-inflammatory effect of rosiglitazone was observed at 24h, but not at 6h, after  $\alpha$ -GalCer administration, suggesting that said effect takes place after regulating the local microenvironment.

To conclude, we identified activated iNKT-like cells at the human maternal-fetal interface in term and preterm gestations. Activated iNKT-like cells were more abundant in the decidual basalis of women who underwent preterm labor than in those who delivered preterm without labor, suggesting that these cells are localized in a fetal antigenic site. The majority (92%) of our samples came from women who underwent spontaneous preterm labor and did not present intra-amniotic infection, which further supports the hypothesis that activated iNKT-like cells are implicated in the sterile process of inflammation that leads to preterm labor/birth.

In summary, this study demonstrates that *in vivo* iNKT-cell activation leads to late preterm labor/birth by activating innate and adaptive immune cells as well as decidual and myometrial cells at the maternal-fetal interface. We also showed that iNKT-cell activation exerts this effect by inducing a maternal systemic pro-inflammatory response. Finally, we demonstrated that PPAR $\gamma$  activation prevents prematurity by modulating the local and systemic inflammatory milieu that accompanies preterm labor. Further exploration of the PPAR $\gamma$  pathway and its regulation in pregnancy complications may lead to novel therapeutic approaches that can improve neonatal outcomes.

## Supplementary Material

Refer to Web version on PubMed Central for supplementary material.

## Acknowledgments

We gratefully acknowledge Amy-Eunice Furcron, Elly N. Sanchez-Rodriguez, Derek Miller, Tara N Mial, Mary Olive, Po Jen (Paul) Chiang, Amapola Balancio, Dr. Zhong Dong, and Lorri McLuckie for their contributions to the execution of this study. We thank the physicians and nurses from the Center for Advanced Obstetrical Care and Research, and the research assistants from the PRB Clinical Laboratory, for their help in collecting human samples. We also thank staff members of the PRB Histology and Pathology Units for their examination of the pathological sections, and Maureen McGerty for her critical readings of the manuscript.

## Non-standard abbreviations

<b><math>\alpha</math>-GalCer</b>	$\alpha$ -galactosylceramide
<b>PPAR<math>\gamma</math></b>	peroxisome proliferator-activated receptor gamma
<b>iNKT</b>	invariant NKT
<b>PTB</b>	preterm birth
<b>dpc</b>	days <i>post coitum</i>

<b>B6</b>	C57BL/6J mice
<b>PTL</b>	preterm labor
<b>PTNL</b>	preterm non-labor
<b>Rosi</b>	rosiglitazone
<b>TIL</b>	term in labor
<b>TNL</b>	term non-labor

## References

1. Liu L, Oza S, Hogan D, Perin J, Rudan I, Lawn JE, Cousens S, Mathers C, Black RE. Global, regional, and national causes of child mortality in 2000–13, with projections to inform post-2015 priorities: an updated systematic analysis. *Lancet*. 2015; 385:430–440. [PubMed: 25280870]
2. Martin JA, Hamilton BE, Osterman MJ, Curtin SC, Matthews TJ. Births: final data for 2013. *Natl Vital Stat Rep*. 2015; 64:1–65.
3. Lubow JM, How HY, Habli M, Maxwell R, Sibai BM. Indications for delivery and short-term neonatal outcomes in late preterm as compared with term births. *Am J Obstet Gynecol*. 2009; 200:e30–33. [PubMed: 19136092]
4. Mwaniki MK, Atieno M, Lawn JE, Newton CR. Long-term neurodevelopmental outcomes after intrauterine and neonatal insults: a systematic review. *Lancet*. 2012; 379:445–452. [PubMed: 22244654]
5. Manuck TA, Sheng X, Yoder BA, Varner MW. Correlation between initial neonatal and early childhood outcomes following preterm birth. *Am J Obstet Gynecol*. 2014; 210:426 e421–429. [PubMed: 24793722]
6. Behrman, RE.; Butler, AS., editors. *Preterm Birth: Causes, Consequences, and Prevention*. Washington (DC): 2007. Societal Costs of Preterm Birth; p. 400
7. Blencowe H, Cousens S, Oestergaard MZ, Chou D, Moller AB, Narwal R, Adler A, Vera Garcia C, Rohde S, Say L, Lawn JE. National, regional, and worldwide estimates of preterm birth rates in the year 2010 with time trends since 1990 for selected countries: a systematic analysis and implications. *Lancet*. 2012; 379:2162–2172. [PubMed: 22682464]
8. Shapiro-Mendoza CK, Lackritz EM. Epidemiology of late and moderate preterm birth. *Semin Fetal Neonatal Med*. 2012; 17:120–125. [PubMed: 22264582]
9. Goldenberg RL, Culhane JF, Iams JD, Romero R. Epidemiology and causes of preterm birth. *Lancet*. 2008; 371:75–84. [PubMed: 18177778]
10. Romero R, Dey SK, Fisher SJ. Preterm labor: one syndrome, many causes. *Science*. 2014; 345:760–765. [PubMed: 25124429]
11. Romero R, Sirtori M, Oyarzun E, Avila C, Mazor M, Callahan R, Sabo V, Athanassiadis AP, Hobbins JC. Infection and labor. V. Prevalence, microbiology, and clinical significance of intraamniotic infection in women with preterm labor and intact membranes. *Am J Obstet Gynecol*. 1989; 161:817–824. [PubMed: 2675611]
12. Romero R, Avila C, Santhanam U, Sehgal PB. Amniotic fluid interleukin 6 in preterm labor. Association with infection. *J Clin Invest*. 1990; 85:1392–1400. [PubMed: 2332497]
13. Romero R, Quintero R, Nores J, Avila C, Mazor M, Hanaoka S, Hagay Z, Merchant L, Hobbins JC. Amniotic fluid white blood cell count: a rapid and simple test to diagnose microbial invasion of the amniotic cavity and predict preterm delivery. *Am J Obstet Gynecol*. 1991; 165:821–830. [PubMed: 1951538]
14. Romero R, Mazor M, Munoz H, Gomez R, Galasso M, Sherer DM. The preterm labor syndrome. *Ann N Y Acad Sci*. 1994; 734:414–429. [PubMed: 7978942]
15. Andrews WW, Hauth JC, Goldenberg RL, Gomez R, Romero R, Cassell GH. Amniotic fluid interleukin-6: correlation with upper genital tract microbial colonization and gestational age in

- women delivered after spontaneous labor versus indicated delivery. *Am J Obstet Gynecol.* 1995; 173:606–612. [PubMed: 7645642]
16. Yoon BH, Jun JK, Park KH, Syn HC, Gomez R, Romero R. Serum C-reactive protein, white blood cell count, and amniotic fluid white blood cell count in women with preterm premature rupture of membranes. *Obstet Gynecol.* 1996; 88:1034–1040. [PubMed: 8942849]
  17. Yoon BH, Chang JW, Romero R. Isolation of *Ureaplasma urealyticum* from the amniotic cavity and adverse outcome in preterm labor. *Obstet Gynecol.* 1998; 92:77–82. [PubMed: 9649098]
  18. Gomez R, Romero R, Ghezzi F, Yoon BH, Mazor M, Berry SM. The fetal inflammatory response syndrome. *Am J Obstet Gynecol.* 1998; 179:194–202. [PubMed: 9704787]
  19. Yoon BH, Romero R, Kim M, Kim EC, Kim T, Park JS, Jun JK. Clinical implications of detection of *Ureaplasma urealyticum* in the amniotic cavity with the polymerase chain reaction. *Am J Obstet Gynecol.* 2000; 183:1130–1137. [PubMed: 11084554]
  20. Romero R, Gomez R, Chaiworapongsa T, Conoscenti G, Kim JC, Kim YM. The role of infection in preterm labour and delivery. *Paediatr Perinat Epidemiol.* 2001; 15(Suppl 2):41–56. [PubMed: 11520399]
  21. Yoon BH, Romero R, Moon JB, Shim SS, Kim M, Kim G, Jun JK. Clinical significance of intra-amniotic inflammation in patients with preterm labor and intact membranes. *Am J Obstet Gynecol.* 2001; 185:1130–1136. [PubMed: 11717646]
  22. Jacobsson B, Mattsby-Baltzer I, Andersch B, Bokstrom H, Holst RM, Wennerholm UB, Hagberg H. Microbial invasion and cytokine response in amniotic fluid in a Swedish population of women in preterm labor. *Acta Obstet Gynecol Scand.* 2003; 82:120–128. [PubMed: 12648172]
  23. Shim SS, Romero R, Hong JS, Park CW, Jun JK, Kim BI, Yoon BH. Clinical significance of intra-amniotic inflammation in patients with preterm premature rupture of membranes. *Am J Obstet Gynecol.* 2004; 191:1339–1345. [PubMed: 15507963]
  24. Romero R, Espinoza J, Goncalves LF, Kusanovic JP, Friel L, Hassan S. The role of inflammation and infection in preterm birth. *Semin Reprod Med.* 2007; 25:21–39. [PubMed: 17205421]
  25. Lee SE, Romero R, Jung H, Park CW, Park JS, Yoon BH. The intensity of the fetal inflammatory response in intraamniotic inflammation with and without microbial invasion of the amniotic cavity. *Am J Obstet Gynecol.* 2007; 197:294 e291–296. [PubMed: 17826426]
  26. Kallapur SG, Kramer BW, Knox CL, Berry CA, Collins JJ, Kemp MW, Nitsos I, Polglase GR, Robinson J, Hillman NH, Newnham JP, Chouhnet C, Jobe AH. Chronic fetal exposure to *Ureaplasma parvum* suppresses innate immune responses in sheep. *J Immunol.* 2011; 187:2688–2695. [PubMed: 21784974]
  27. Cobo T, Palacio M, Martinez-Terron M, Navarro-Sastre A, Bosch J, Filella X, Gratacos E. Clinical and inflammatory markers in amniotic fluid as predictors of adverse outcomes in preterm premature rupture of membranes. *Am J Obstet Gynecol.* 2011; 205:126 e121–128. [PubMed: 21621184]
  28. Agrawal V, Hirsch E. Intrauterine infection and preterm labor. *Semin Fetal Neonatal Med.* 2012; 17:12–19. [PubMed: 21944863]
  29. Romero R, Miranda J, Chaiworapongsa T, Chaemsaitong P, Gotsch F, Dong Z, Ahmed AI, Yoon BH, Hassan SS, Kim CJ, Korzeniewski SJ, Yeo L, Kim YM. Sterile intra-amniotic inflammation in asymptomatic patients with a sonographic short cervix: prevalence and clinical significance. *J Matern Fetal Neonatal Med.* 2014:1–17.
  30. Romero R, Miranda J, Chaiworapongsa T, Korzeniewski SJ, Chaemsaitong P, Gotsch F, Dong Z, Ahmed AI, Yoon BH, Hassan SS, Kim CJ, Yeo L. Prevalence and Clinical Significance of Sterile Intra-amniotic Inflammation in Patients with Preterm Labor and Intact Membranes. *Am J Reprod Immunol.* 2014; 72:458–472. [PubMed: 25078709]
  31. Romero R, Miranda J, Chaiworapongsa T, Chaemsaitong P, Gotsch F, Dong Z, Ahmed AI, Yoon BH, Hassan SS, Kim CJ, Korzeniewski SJ, Yeo L. A novel molecular microbiologic technique for the rapid diagnosis of microbial invasion of the amniotic cavity and intra-amniotic infection in preterm labor with intact membranes. *Am J Reprod Immunol.* 2014; 71:330–358. [PubMed: 24417618]
  32. Romero R, Miranda J, Chaemsaitong P, Chaiworapongsa T, Kusanovic JP, Dong Z, Ahmed AI, Shaman M, Lannaman K, Yoon BH, Hassan SS, Kim CJ, Korzeniewski SJ, Yeo L, Kim YM.

- Sterile and microbial-associated intra-amniotic inflammation in preterm prelabor rupture of membranes. *J Matern Fetal Neonatal Med.* 2014;1–16.
33. Combs CA, Gravett M, Garite TJ, Hickok DE, Lapidus J, Porreco R, Rael J, Grove T, Morgan TK, Clewell W, Miller H, Luthy D, Pereira L, Nageotte M, Robilio PA, Fortunato S, Simhan H, Baxter JK, Amon E, Franco A, Trofatter K, Heyborne K. ProteoGenix/Obstetrix Collaborative Research N. Amniotic fluid infection, inflammation, and colonization in preterm labor with intact membranes. *Am J Obstet Gynecol.* 2014; 210:125 e121–125 e115. [PubMed: 24274987]
  34. Kacerovsky M, Musilova I, Andrys C, Hornychova H, Pliskova L, Kostal M, Jacobsson B. Prelabor rupture of membranes between 34 and 37 weeks: the intraamniotic inflammatory response and neonatal outcomes. *Am J Obstet Gynecol.* 2014; 210:325 e321–325 e310. [PubMed: 24184182]
  35. Gervasi MT, Chaiworapongsa T, Naccasha N, Blackwell S, Yoon BH, Maymon E, Romero R. Phenotypic and metabolic characteristics of maternal monocytes and granulocytes in preterm labor with intact membranes. *Am J Obstet Gynecol.* 2001; 185:1124–1129. [PubMed: 11717645]
  36. Gervasi MT, Chaiworapongsa T, Naccasha N, Pacora P, Berman S, Maymon E, Kim JC, Kim YM, Yoshimatsu J, Espinoza J, Romero R. Maternal intravascular inflammation in preterm premature rupture of membranes. *J Matern Fetal Neonatal Med.* 2002; 11:171–175. [PubMed: 12380672]
  37. Mittal P, Romero R, Tarca AL, Draghici S, Nhan-Chang CL, Chaiworapongsa T, Hotra J, Gomez R, Kusanovic JP, Lee DC, Kim CJ, Hassan SS. A molecular signature of an arrest of descent in human parturition. *Am J Obstet Gynecol.* 2011; 204:177 e115–133. [PubMed: 21284969]
  38. Chaemsaitong P, Madan I, Romero R, Than NG, Tarca AL, Draghici S, Bhatti G, Yeo L, Mazor M, Kim CJ, Hassan SS, Chaiworapongsa T. Characterization of the myometrial transcriptome in women with an arrest of dilatation during labor. *J Perinat Med.* 2013; 41:665–681. [PubMed: 23893668]
  39. Kim YM, Romero R, Chaiworapongsa T, Kim GJ, Kim MR, Kuivaniemi H, Tromp G, Espinoza J, Bujold E, Abrahams VM, Mor G. Toll-like receptor-2 and -4 in the chorioamniotic membranes in spontaneous labor at term and in preterm parturition that are associated with chorioamnionitis. *Am J Obstet Gynecol.* 2004; 191:1346–1355. [PubMed: 15507964]
  40. Murphy SP, Hanna NN, Fast LD, Shaw SK, Berg G, Padbury JF, Romero R, Sharma S. Evidence for participation of uterine natural killer cells in the mechanisms responsible for spontaneous preterm labor and delivery. *Am J Obstet Gynecol.* 2009; 200:308 e301–309. [PubMed: 19114277]
  41. Koga K, Cardenas I, Aldo P, Abrahams VM, Peng B, Fill S, Romero R, Mor G. Activation of TLR3 in the trophoblast is associated with preterm delivery. *Am J Reprod Immunol.* 2009; 61:196–212. [PubMed: 19239422]
  42. Cardenas I, Means RE, Aldo P, Koga K, Lang SM, Booth CJ, Manzur A, Oyarzun E, Romero R, Mor G. Viral infection of the placenta leads to fetal inflammation and sensitization to bacterial products predisposing to preterm labor. *J Immunol.* 2010; 185:1248–1257. [PubMed: 20554966]
  43. Cardenas I, Mulla MJ, Myrtolli K, Sfakianaki AK, Norwitz ER, Tadesse S, Guller S, Abrahams VM. Nod1 activation by bacterial iE-DAP induces maternal-fetal inflammation and preterm labor. *J Immunol.* 2011; 187:980–986. [PubMed: 21677137]
  44. Romero R, Chaiworapongsa T, Alpay Savasan Z, Xu Y, Hussein Y, Dong Z, Kusanovic JP, Kim CJ, Hassan SS. Damage-associated molecular patterns (DAMPs) in preterm labor with intact membranes and preterm PROM: a study of the alarmin HMGB1. *J Matern Fetal Neonatal Med.* 2011; 24:1444–1455. [PubMed: 21958433]
  45. Jaiswal MK, Agrawal V, Mallers T, Gilman-Sachs A, Hirsch E, Beaman KD. Regulation of apoptosis and innate immune stimuli in inflammation-induced preterm labor. *J Immunol.* 2013; 191:5702–5713. [PubMed: 24163412]
  46. Shynlova O, Nedd-Roderique T, Li Y, Dorogin A, Lye SJ. Myometrial immune cells contribute to term parturition, preterm labour and post-partum involution in mice. *J Cell Mol Med.* 2013; 17:90–102. [PubMed: 23205502]
  47. Arenas-Hernandez M, Romero R, St Louis D, Hassan SS, Kaye EB, Gomez-Lopez N. An imbalance between innate and adaptive immune cells at the maternal-fetal interface occurs prior to endotoxin-induced preterm birth. *Cell Mol Immunol.* 2015 In press.

48. Thaxton JE, Nevers TA, Sharma S. TLR-mediated preterm birth in response to pathogenic agents. *Infect Dis Obstet Gynecol.* 2010; 2010
49. Friel LA, Romero R, Edwin S, Nien JK, Gomez R, Chaiworapongsa T, Kusanovic JP, Tolosa JE, Hassan SS, Espinoza J. The calcium binding protein, S100B, is increased in the amniotic fluid of women with intra-amniotic infection/inflammation and preterm labor with intact or ruptured membranes. *J Perinat Med.* 2007; 35:385–393. [PubMed: 17624933]
50. Romero R, Espinoza J, Hassan S, Gotsch F, Kusanovic JP, Avila C, Erez O, Edwin S, Schmidt AM. Soluble receptor for advanced glycation end products (sRAGE) and endogenous secretory RAGE (esRAGE) in amniotic fluid: modulation by infection and inflammation. *J Perinat Med.* 2008; 36:388–398. [PubMed: 18593373]
51. Chaiworapongsa T, Erez O, Kusanovic JP, Vaisbuch E, Mazaki-Tovi S, Gotsch F, Than NG, Mittal P, Kim YM, Camacho N, Edwin S, Gomez R, Hassan SS, Romero R. Amniotic fluid heat shock protein 70 concentration in histologic chorioamnionitis, term and preterm parturition. *J Matern Fetal Neonatal Med.* 2008; 21:449–461. [PubMed: 18570125]
52. Lee SE, Park IS, Romero R, Yoon BH. Amniotic fluid prostaglandin F2 increases even in sterile amniotic fluid and is an independent predictor of impending delivery in preterm premature rupture of membranes. *J Matern Fetal Neonatal Med.* 2009; 22:880–886. [PubMed: 19544157]
53. Lotze MT, Deisseroth A, Rubartelli A. Damage associated molecular pattern molecules. *Clin Immunol.* 2007; 124:1–4. [PubMed: 17468050]
54. Oppenheim JJ, Yang D. Alarmins: chemotactic activators of immune responses. *Curr Opin Immunol.* 2005; 17:359–365. [PubMed: 15955682]
55. Chen GY, Nunez G. Sterile inflammation: sensing and reacting to damage. *Nat Rev Immunol.* 2010; 10:826–837. [PubMed: 21088683]
56. Espinoza J, Romero R, Chaiworapongsa T, Kim JC, Yoshimatsu J, Edwin S, Rathnasabapathy C, Tolosa J, Donnenfeld A, Craparo F, Gomez R, Bujold E. Lipopolysaccharide-binding protein in microbial invasion of the amniotic cavity and human parturition. *J Matern Fetal Neonatal Med.* 2002; 12:313–321. [PubMed: 12607763]
57. Romero R, Miranda J, Chaemsathong P, Chaiworapongsa T, Kusanovic JP, Dong Z, Ahmed AI, Shaman M, Lannaman K, Yoon BH, Hassan SS, Kim CJ, Korzeniewski SJ, Yeo L, Kim YM. Sterile and microbial-associated intra-amniotic inflammation in preterm prelabor rupture of membranes. *J Matern Fetal Neonatal Med.* 2015; 28:1394–1409. [PubMed: 25190175]
58. Romero R, Mazor M, Tartakovsky B. Systemic administration of interleukin-1 induces preterm parturition in mice. *Am J Obstet Gynecol.* 1991; 165:969–971. [PubMed: 1951564]
59. Gomez-Lopez N, Romero R, Plazyo O, Panaitescu B, Furcron AE, Miller D, Roumayah T, Flom E, Hassan SA. Intra-amniotic administration of HMGB1 induces spontaneous preterm labor and birth. *Am J Reprod Immunol.* 2015 In press.
60. Cayrol C, Girard JP. The IL-1-like cytokine IL-33 is inactivated after maturation by caspase-1. *Proc Natl Acad Sci U S A.* 2009; 106:9021–9026. [PubMed: 19439663]
61. Topping V, Romero R, Than NG, Tarca AL, Xu Z, Kim SY, Wang B, Yeo L, Kim CJ, Hassan SS, Kim JS. Interleukin-33 in the human placenta. *J Matern Fetal Neonatal Med.* 2013; 26:327–338. [PubMed: 23039129]
62. Kim CJ, Romero R, Chaemsathong P, Chaiyasit N, Yoon BH, Kim YM. Acute chorioamnionitis and funisitis: definition, pathologic features, and clinical significance. *Am J Obstet Gynecol.* 2015; 213:S29–52. [PubMed: 26428501]
63. Bourgeois E, Van LP, Samson M, Diem S, Barra A, Roga S, Gombert JM, Schneider E, Dy M, Gourdy P, Girard JP, Herbelin A. The pro-Th2 cytokine IL-33 directly interacts with invariant NKT and NK cells to induce IFN-gamma production. *Eur J Immunol.* 2009; 39:1046–1055. [PubMed: 19266498]
64. Smithgall MD, Comeau MR, Yoon BR, Kaufman D, Armitage R, Smith DE. IL-33 amplifies both Th1- and Th2-type responses through its activity on human basophils, allergen-reactive Th2 cells, iNKT and NK cells. *Int Immunol.* 2008; 20:1019–1030. [PubMed: 18550585]
65. Kitamura H, Iwakabe K, Yahata T, Nishimura S, Ohta A, Ohmi Y, Sato M, Takeda K, Okumura K, Van Kaer L, Kawano T, Taniguchi M, Nishimura T. The natural killer T (NKT) cell ligand alpha-galactosylceramide demonstrates its immunopotentiating effect by inducing interleukin (IL)-12

- production by dendritic cells and IL-12 receptor expression on NKT cells. *J Exp Med*. 1999; 189:1121–1128. [PubMed: 10190903]
66. Tomura M, Yu WG, Ahn HJ, Yamashita M, Yang YF, Ono S, Hamaoka T, Kawano T, Taniguchi M, Koezuka Y, Fujiwara H. A novel function of Valpha14+CD4+NKT cells: stimulation of IL-12 production by antigen-presenting cells in the innate immune system. *J Immunol*. 1999; 163:93–101. [PubMed: 10384104]
67. Fujii S, Shimizu K, Kronenberg M, Steinman RM. Prolonged IFN-gamma-producing NKT response induced with alpha-galactosylceramide-loaded DCs. *Nat Immunol*. 2002; 3:867–874. [PubMed: 12154358]
68. Brigl M, Bry L, Kent SC, Gumperz JE, Brenner MB. Mechanism of CD1d-restricted natural killer T cell activation during microbial infection. *Nat Immunol*. 2003; 4:1230–1237. [PubMed: 14578883]
69. Oki S, Chiba A, Yamamura T, Miyake S. The clinical implication and molecular mechanism of preferential IL-4 production by modified glycolipid-stimulated NKT cells. *J Clin Invest*. 2004; 113:1631–1640. [PubMed: 15173890]
70. Sag D, Krause P, Hedrick CC, Kronenberg M, Wingender G. IL-10-producing NKT10 cells are a distinct regulatory invariant NKT cell subset. *J Clin Invest*. 2014; 124:3725–3740. [PubMed: 25061873]
71. Bendelac A, Savage PB, Teyton L. The biology of NKT cells. *Annu Rev Immunol*. 2007; 25:297–336. [PubMed: 17150027]
72. Kawano T, Cui J, Koezuka Y, Toura I, Kaneko Y, Motoki K, Ueno H, Nakagawa R, Sato H, Kondo E, Koseki H, Taniguchi M. CD1d-restricted and TCR-mediated activation of valpha14 NKT cells by glycosylceramides. *Science*. 1997; 278:1626–1629. [PubMed: 9374463]
73. Sidobre S, Naidenko OV, Sim BC, Gascoigne NR, Garcia KC, Kronenberg M. The V alpha 14 NKT cell TCR exhibits high-affinity binding to a glycolipid/CD1d complex. *J Immunol*. 2002; 169:1340–1348. [PubMed: 12133957]
74. Lehmann JM, Moore LB, Smith-Oliver TA, Wilkison WO, Willson TM, Kliewer SA. An antidiabetic thiazolidinedione is a high affinity ligand for peroxisome proliferator-activated receptor gamma (PPAR gamma). *J Biol Chem*. 1995; 270:12953–12956. [PubMed: 7768881]
75. Ricote M, Li AC, Willson TM, Kelly CJ, Glass CK. The peroxisome proliferator-activated receptor-gamma is a negative regulator of macrophage activation. *Nature*. 1998; 391:79–82. [PubMed: 9422508]
76. Chinetti G, Griglio S, Antonucci M, Torra IP, Delerive P, Majd Z, Fruchart JC, Chapman J, Najib J, Staels B. Activation of proliferator-activated receptors alpha and gamma induces apoptosis of human monocyte-derived macrophages. *J Biol Chem*. 1998; 273:25573–25580. [PubMed: 9748221]
77. Delerive P, Martin-Nizard F, Chinetti G, Trottein F, Fruchart JC, Najib J, Duriez P, Staels B. Peroxisome proliferator-activated receptor activators inhibit thrombin-induced endothelin-1 production in human vascular endothelial cells by inhibiting the activator protein-1 signaling pathway. *Circ Res*. 1999; 85:394–402. [PubMed: 10473669]
78. McCarthy FP, Delany AC, Kenny LC, Walsh SK. PPAR-gamma -- a possible drug target for complicated pregnancies. *Br J Pharmacol*. 2013; 168:1074–1085. [PubMed: 23186152]
79. Forman BM, Tontonoz P, Chen J, Brun RP, Spiegelman BM, Evans RM. 15-Deoxy-delta 12, 14-prostaglandin J2 is a ligand for the adipocyte determination factor PPAR gamma. *Cell*. 1995; 83:803–812. [PubMed: 8521497]
80. Kliewer SA, Lenhard JM, Willson TM, Patel I, Morris DC, Lehmann JM. A prostaglandin J2 metabolite binds peroxisome proliferator-activated receptor gamma and promotes adipocyte differentiation. *Cell*. 1995; 83:813–819. [PubMed: 8521498]
81. Pirianov G, Waddington SN, Lindstrom TM, Terzidou V, Mehmet H, Bennett PR. The cyclopentenone 15-deoxy-delta 12,14-prostaglandin J(2) delays lipopolysaccharide-induced preterm delivery and reduces mortality in the newborn mouse. *Endocrinology*. 2009; 150:699–706. [PubMed: 18845626]

82. Arenas-Hernandez M, Sanchez-Rodriguez EN, Mial NT, Robertson SA, Gomez-Lopez N. Isolation of leukocytes from the murine tissues at the maternal-fetal interface. *J Vis Exp*. 2015; 99:e52866. [PubMed: 26067389]
83. ACOG Practice Bulletin Number 49, December 2003: Dystocia and augmentation of labor. *Obstet Gynecol*. 2003; 102:1445–1454. [PubMed: 14662243]
84. Redline RW. Placental pathology: a systematic approach with clinical correlations. *Placenta*. 2008; 29(Suppl A):S86–91. [PubMed: 17950457]
85. Kim CJ, Romero R, Kusanovic JP, Yoo W, Dong Z, Topping V, Gotsch F, Yoon BH, Chi JG, Kim JS. The frequency, clinical significance, and pathological features of chronic chorioamnionitis: a lesion associated with spontaneous preterm birth. *Mod Pathol*. 2010; 23:1000–1011. [PubMed: 20348884]
86. Xu Y, Plazyo O, Romero R, Hassan SS, Gomez-Lopez N. Isolation of leukocytes from the human maternal-fetal interface. *J Vis Exp*. 2015; 99:e52863. [PubMed: 26067211]
87. Rochelson BL, Schulman H, Fleischer A, Farmakides G, Bracero L, Ducey J, Winter D, Penny B. The clinical significance of Doppler umbilical artery velocimetry in the small for gestational age fetus. *Am J Obstet Gynecol*. 1987; 156:1223–1226. [PubMed: 2953246]
88. Schulman H. The clinical implications of Doppler ultrasound analysis of the uterine and umbilical arteries. *Am J Obstet Gynecol*. 1987; 156:889–893. [PubMed: 2953241]
89. ACOG technical bulletin. Fetal heart rate patterns: monitoring, interpretation, and management. Number 207--July 1995 (replaces No. 132, September 1989). *Int J Gynaecol Obstet*. 1995; 51:65–74. [PubMed: 8582524]
90. Electronic fetal heart rate monitoring: research guidelines for interpretation. The National Institute of Child Health and Human Development Research Planning Workshop. *J Obstet Gynecol Neonatal Nurs*. 1997; 26:635–640.
91. Boyson JE, Nagarkatti N, Nizam L, Exley MA, Strominger JL. Gestation stage-dependent mechanisms of invariant natural killer T cell-mediated pregnancy loss. *Proc Natl Acad Sci U S A*. 2006; 103:4580–4585. [PubMed: 16537414]
92. Ito K, Karasawa M, Kawano T, Akasaka T, Koseki H, Akutsu Y, Kondo E, Sekiya S, Sekikawa K, Harada M, Yamashita M, Nakayama T, Taniguchi M. Involvement of decidual Valpha14 NKT cells in abortion. *Proc Natl Acad Sci U S A*. 2000; 97:740–744. [PubMed: 10639149]
93. Szatmari I, Gogolak P, Im JS, Dezso B, Rajnavolgyi E, Nagy L. Activation of PPARgamma specifies a dendritic cell subtype capable of enhanced induction of iNKT cell expansion. *Immunity*. 2004; 21:95–106. [PubMed: 15345223]
94. Frohnert BI, Hui TY, Bernlohr DA. Identification of a functional peroxisome proliferator-responsive element in the murine fatty acid transport protein gene. *J Biol Chem*. 1999; 274:3970–3977. [PubMed: 9933587]
95. Chiu YH, Jayawardena J, Weiss A, Lee D, Park SH, Dautry-Varsat A, Bendelac A. Distinct subsets of CD1d-restricted T cells recognize self-antigens loaded in different cellular compartments. *J Exp Med*. 1999; 189:103–110. [PubMed: 9874567]
96. Crowe NY, Coquet JM, Berzins SP, Kyparissoudis K, Keating R, Pellicci DG, Hayakawa Y, Godfrey DI, Smyth MJ. Differential antitumor immunity mediated by NKT cell subsets in vivo. *J Exp Med*. 2005; 202:1279–1288. [PubMed: 16275765]
97. Terabe M, Swann J, Ambrosino E, Sinha P, Takaku S, Hayakawa Y, Godfrey DI, Ostrand-Rosenberg S, Smyth MJ, Berzofsky JA. A nonclassical non-Valpha14Jalpha18 CD1d-restricted (type II) NKT cell is sufficient for down-regulation of tumor immunosurveillance. *J Exp Med*. 2005; 202:1627–1633. [PubMed: 16365146]
98. Zheng Q, Zhou L, Mi QS. MicroRNA miR-150 is involved in Valpha14 invariant NKT cell development and function. *J Immunol*. 2012; 188:2118–2126. [PubMed: 22287707]
99. Taniguchi M, Seino K, Nakayama T. The NKT cell system: bridging innate and acquired immunity. *Nat Immunol*. 2003; 4:1164–1165. [PubMed: 14639465]
100. Carnaud C, Lee D, Donnars O, Park SH, Beavis A, Koezuka Y, Bendelac A. Cutting edge: Cross-talk between cells of the innate immune system: NKT cells rapidly activate NK cells. *J Immunol*. 1999; 163:4647–4650. [PubMed: 10528160]

101. Singh N, Hong S, Scherer DC, Serizawa I, Burdin N, Kronenberg M, Koezuka Y, Van Kaer L. Cutting edge: activation of NK T cells by CD1d and alpha-galactosylceramide directs conventional T cells to the acquisition of a Th2 phenotype. *J Immunol.* 1999; 163:2373–2377. [PubMed: 10452969]
102. Nishimura T, Kitamura H, Iwakabe K, Yahata T, Ohta A, Sato M, Takeda K, Okumura K, Van Kaer L, Kawano T, Taniguchi M, Nakui M, Sekimoto M, Koda T. The interface between innate and acquired immunity: glycolipid antigen presentation by CD1d-expressing dendritic cells to NKT cells induces the differentiation of antigen-specific cytotoxic T lymphocytes. *Int Immunol.* 2000; 12:987–994. [PubMed: 10882410]
103. Kitamura H, Ohta A, Sekimoto M, Sato M, Iwakabe K, Nakui M, Yahata T, Meng H, Koda T, Nishimura S, Kawano T, Taniguchi M, Nishimura T. alpha-galactosylceramide induces early B-cell activation through IL-4 production by NKT cells. *Cell Immunol.* 2000; 199:37–42. [PubMed: 10675273]
104. Wang H, Feng D, Park O, Yin S, Gao B. Invariant NKT cell activation induces neutrophil accumulation and hepatitis: opposite regulation by IL-4 and IFN-gamma. *Hepatology.* 2013; 58:1474–1485. [PubMed: 23686838]
105. Fujii S, Shimizu K, Smith C, Bonifaz L, Steinman RM. Activation of natural killer T cells by alpha-galactosylceramide rapidly induces the full maturation of dendritic cells in vivo and thereby acts as an adjuvant for combined CD4 and CD8 T cell immunity to a coadministered protein. *J Exp Med.* 2003; 198:267–279. [PubMed: 12874260]
106. Xue J, Schmidt SV, Sander J, Draffehn A, Krebs W, Quester I, De Nardo D, Gohel TD, Emde M, Schmidleithner L, Ganesan H, Nino-Castro A, Mallmann MR, Labzin L, Theis H, Kraut M, Beyer M, Latz E, Freeman TC, Ulas T, Schultze JL. Transcriptome-based network analysis reveals a spectrum model of human macrophage activation. *Immunity.* 2014; 40:274–288. [PubMed: 24530056]
107. Murray PJ, Allen JE, Biswas SK, Fisher EA, Gilroy DW, Goerdt S, Gordon S, Hamilton JA, Ivashkiv LB, Lawrence T, Locati M, Mantovani A, Martinez FO, Mege JL, Mosser DM, Natoli G, Saeij JP, Schultze JL, Shirey KA, Sica A, Suttles J, Udalova I, van Ginderachter JA, Vogel SN, Wynn TA. Macrophage activation and polarization: nomenclature and experimental guidelines. *Immunity.* 2014; 41:14–20. [PubMed: 25035950]
108. Mills CD, Kincaid K, Alt JM, Heilman MJ, Hill AM. M-1/M-2 macrophages and the Th1/Th2 paradigm. *J Immunol.* 2000; 164:6166–6173. [PubMed: 10843666]
109. Mantovani A, Sozzani S, Locati M, Allavena P, Sica A. Macrophage polarization: tumor-associated macrophages as a paradigm for polarized M2 mononuclear phagocytes. *Trends Immunol.* 2002; 23:549–555. [PubMed: 12401408]
110. Biswas SK, Mantovani A. Macrophage plasticity and interaction with lymphocyte subsets: cancer as a paradigm. *Nat Immunol.* 2010; 11:889–896. [PubMed: 20856220]
111. Sica A, Mantovani A. Macrophage plasticity and polarization: in vivo veritas. *J Clin Invest.* 2012; 122:787–795. [PubMed: 22378047]
112. Ellis TN, Beaman BL. Murine polymorphonuclear neutrophils produce interferon-gamma in response to pulmonary infection with *Nocardia asteroides*. *J Leukoc Biol.* 2002; 72:373–381. [PubMed: 12149429]
113. Ethuin F, Gerard B, Benna JE, Boutten A, Gougereot-Pocidal MA, Jacob L, Chollet-Martin S. Human neutrophils produce interferon gamma upon stimulation by interleukin-12. *Lab Invest.* 2004; 84:1363–1371. [PubMed: 15220936]
114. Boyson JE, Rybalov B, Koopman LA, Exley M, Balk SP, Racke FK, Schatz F, Masch R, Wilson SB, Strominger JL. CD1d and invariant NKT cells at the human maternal-fetal interface. *Proc Natl Acad Sci U S A.* 2002; 99:13741–13746. [PubMed: 12368486]
115. Li LP, Fang YC, Dong GF, Lin Y, Saito S. Depletion of invariant NKT cells reduces inflammation-induced preterm delivery in mice. *J Immunol.* 2012; 188:4681–4689. [PubMed: 22467647]
116. Li L, Yang J, Jiang Y, Tu J, Schust DJ. Activation of decidual invariant natural killer T cells promotes lipopolysaccharide-induced preterm birth. *Mol Hum Reprod.* 2015; 21:369–381. [PubMed: 25589517]



117. Mattner J, Debord KL, Ismail N, Goff RD, Cantu C 3rd, Zhou D, Saint-Mezard P, Wang V, Gao Y, Yin N, Hoebe K, Schneewind O, Walker D, Beutler B, Teyton L, Savage PB, Bendelac A. Exogenous and endogenous glycolipid antigens activate NKT cells during microbial infections. *Nature*. 2005; 434:525–529. [PubMed: 15791258]
118. Aluvihare VR, Kallikourdis M, Betz AG. Regulatory T cells mediate maternal tolerance to the fetus. *Nat Immunol*. 2004; 5:266–271. [PubMed: 14758358]
119. Rowe JH, Ertelt JM, Xin L, Way SS. Pregnancy imprints regulatory memory that sustains anergy to fetal antigen. *Nature*. 2012; 490:102–106. [PubMed: 23023128]
120. Shima T, Sasaki Y, Itoh M, Nakashima A, Ishii N, Sugamura K, Saito S. Regulatory T cells are necessary for implantation and maintenance of early pregnancy but not late pregnancy in allogeneic mice. *J Reprod Immunol*. 2010; 85:121–129. [PubMed: 20439117]
121. Wang ML, Dorer DJ, Fleming MP, Catlin EA. Clinical outcomes of near-term infants. *Pediatrics*. 2004; 114:372–376. [PubMed: 15286219]
122. Raju TN, Higgins RD, Stark AR, Leveno KJ. Optimizing care and outcome for late-preterm (near-term) infants: a summary of the workshop sponsored by the National Institute of Child Health and Human Development. *Pediatrics*. 2006; 118:1207–1214. [PubMed: 16951017]
123. Pellicci DG, Hammond KJ, Uldrich AP, Baxter AG, Smyth MJ, Godfrey DI. A natural killer T (NKT) cell developmental pathway involving a thymus-dependent NK1.1(–)CD4(+) CD1d-dependent precursor stage. *J Exp Med*. 2002; 195:835–844. [PubMed: 11927628]
124. Dunn-Albanese LR, Ackerman WE, Xie Y, Iams JD, Kniss DA. Reciprocal expression of peroxisome proliferator-activated receptor-gamma and cyclooxygenase-2 in human term parturition. *Am J Obstet Gynecol*. 2004; 190:809–816. [PubMed: 15042019]
125. Mial NT, Kadam L, Romero R, Drewlo S, Gomez-Lopez N. Rosiglitazone treatment rapidly controls the systemic pro-inflammatory response and reduces the rate of infection-induced preterm birth. *Reprod Sci*. 2015; 22:137A.
126. Crowe NY, Uldrich AP, Kyparissoudis K, Hammond KJ, Hayakawa Y, Sidobre S, Keating R, Kronenberg M, Smyth MJ, Godfrey DI. Glycolipid antigen drives rapid expansion and sustained cytokine production by NK T cells. *J Immunol*. 2003; 171:4020–4027. [PubMed: 14530322]
127. Szatmari I, Pap A, Ruhl R, Ma JX, Illarionov PA, Besra GS, Rajnavolgyi E, Dezso B, Nagy L. PPARgamma controls CD1d expression by turning on retinoic acid synthesis in developing human dendritic cells. *J Exp Med*. 2006; 203:2351–2362. [PubMed: 16982809]
128. Brossay L, Jullien D, Cardell S, Sydora BC, Burdin N, Modlin RL, Kronenberg M. Mouse CD1 is mainly expressed on hemopoietic-derived cells. *J Immunol*. 1997; 159:1216–1224. [PubMed: 9233616]
129. Roark JH, Park SH, Jayawardena J, Kavita U, Shannon M, Bendelac A. CD1.1 expression by mouse antigen-presenting cells and marginal zone B cells. *J Immunol*. 1998; 160:3121–3127. [PubMed: 9531266]
130. Bendelac A. Positive selection of mouse NK1+ T cells by CD1-expressing cortical thymocytes. *J Exp Med*. 1995; 182:2091–2096. [PubMed: 7500054]
131. Gomez-Lopez N, Guilbert LJ, Olson DM. Invasion of the leukocytes into the fetal-maternal interface during pregnancy. *J Leukoc Biol*. 2010; 88:625–633. [PubMed: 20519637]
132. Gomez-Lopez N, StLouis D, Lehr MA, Sanchez-Rodriguez EN, Arenas-Hernandez M. Immune cells in term and preterm labor. *Cell Mol Immunol*. 2014
133. Bizargity P, Del Rio R, Phillippe M, Teuscher C, Bonney EA. Resistance to lipopolysaccharide-induced preterm delivery mediated by regulatory T cell function in mice. *Biol Reprod*. 2009; 80:874–881. [PubMed: 19144956]
134. Gomez-Lopez N, Vadillo-Perez L, Hernandez-Carbajal A, Godines-Enriquez M, Olson DM, Vadillo-Ortega F. Specific inflammatory microenvironments in the zones of the fetal membranes at term delivery. *Am J Obstet Gynecol*. 2011; 205:235 e215–224. [PubMed: 21763637]
135. Gomez-Lopez N, Vega-Sanchez R, Castillo-Castrejon M, Romero R, Cubeiro-Arreola K, Vadillo-Ortega F. Evidence for a role for the adaptive immune response in human term parturition. *Am J Reprod Immunol*. 2013; 69:212–230. [PubMed: 23347265]
136. Gomez-Lopez N, Olson DM, Robertson SA. Interleukin-6 controls uterine Th9 cells and CD8 T regulatory cells to accelerate parturition in mice. *Immunol Cell Biol*. 2015

137. Marx N, Kehrle B, Kohlhammer K, Grub M, Koenig W, Hombach V, Libby P, Plutzky J. PPAR activators as antiinflammatory mediators in human T lymphocytes: implications for atherosclerosis and transplantation-associated arteriosclerosis. *Circ Res.* 2002; 90:703–710. [PubMed: 11934839]
138. Yang XY, Wang LH, Chen T, Hodge DR, Resau JH, DaSilva L, Farrar WL. Activation of human T lymphocytes is inhibited by peroxisome proliferator-activated receptor gamma (PPARgamma) agonists. PPARgamma co-association with transcription factor NFAT. *J Biol Chem.* 2000; 275:4541–4544. [PubMed: 10671476]
139. Gonzalez JM, Franzke CW, Yang F, Romero R, Girardi G. Complement activation triggers metalloproteinases release inducing cervical remodeling and preterm birth in mice. *Am J Pathol.* 2011; 179:838–849. [PubMed: 21801872]
140. Jiang C, Ting AT, Seed B. PPAR-gamma agonists inhibit production of monocyte inflammatory cytokines. *Nature.* 1998; 391:82–86. [PubMed: 9422509]
141. Kintscher U, Goetze S, Wakino S, Kim S, Nagpal S, Chandraratna RA, Graf K, Fleck E, Hsueh WA, Law RE. Peroxisome proliferator-activated receptor and retinoid X receptor ligands inhibit monocyte chemotactic protein-1-directed migration of monocytes. *Eur J Pharmacol.* 2000; 401:259–270. [PubMed: 10936484]
142. Rinaldi SF, Catalano RD, Wade J, Rossi AG, Norman JE. Decidual neutrophil infiltration is not required for preterm birth in a mouse model of infection-induced preterm labor. *J Immunol.* 2014; 192:2315–2325. [PubMed: 24501200]
143. Reddy RC, Narala VR, Keshamouni VG, Milam JE, Newstead MW, Standiford TJ. Sepsis-induced inhibition of neutrophil chemotaxis is mediated by activation of peroxisome proliferator-activated receptor- $\gamma$ . *Blood.* 2008; 112:4250–4258. [PubMed: 18535203]
144. Blois SM, Alba Soto CD, Tometten M, Klapp BF, Margni RA, Arck PC. Lineage, maturity, and phenotype of uterine murine dendritic cells throughout gestation indicate a protective role in maintaining pregnancy. *Biol Reprod.* 2004; 70:1018–1023. [PubMed: 14681197]
145. Bizargity P, Bonney EA. Dendritic cells: a family portrait at mid-gestation. *Immunology.* 2009; 126:565–578. [PubMed: 18778288]
146. Faveeuw C, Fougeray S, Angeli V, Fontaine J, Chinetti G, Gosset P, Delerive P, Maliszewski C, Capron M, Staels B, Moser M, Trottein F. Peroxisome proliferator-activated receptor gamma activators inhibit interleukin-12 production in murine dendritic cells. *FEBS Lett.* 2000; 486:261–266. [PubMed: 11119715]
147. Romero R, Manogue KR, Mitchell MD, Wu YK, Oyarzun E, Hobbins JC, Cerami A. Infection and labor. IV. Cachectin-tumor necrosis factor in the amniotic fluid of women with intraamniotic infection and preterm labor. *Am J Obstet Gynecol.* 1989; 161:336–341. [PubMed: 2764054]
148. Casey ML, Cox SM, Beutler B, Milewich L, MacDonald PC. Cachectin/tumor necrosis factor-alpha formation in human decidua. Potential role of cytokines in infection-induced preterm labor. *J Clin Invest.* 1989; 83:430–436. [PubMed: 2913048]
149. Romero R, Mazor M, Sepulveda W, Avila C, Copeland D, Williams J. Tumor necrosis factor in preterm and term labor. *Am J Obstet Gynecol.* 1992; 166:1576–1587. [PubMed: 1595815]
150. Jacobsson B, Holst RM, Wennerholm UB, Andersson B, Lilja H, Hagberg H. Monocyte chemotactic protein-1 in cervical and amniotic fluid: relationship to microbial invasion of the amniotic cavity, intra-amniotic inflammation, and preterm delivery. *Am J Obstet Gynecol.* 2003; 189:1161–1167. [PubMed: 14586371]
151. Esplin MS, Peltier MR, Hamblin S, Smith S, Fausett MB, Dildy GA, Branch DW, Silver RM, Adashi EY. Monocyte chemotactic protein-1 expression is increased in human gestational tissues during term and preterm labor. *Placenta.* 2005; 26:661–671. [PubMed: 16085045]
152. Esplin MS, Romero R, Chaiworapongsa T, Kim YM, Edwin S, Gomez R, Mazor M, Adashi EY. Monocyte chemotactic protein-1 is increased in the amniotic fluid of women who deliver preterm in the presence or absence of intra-amniotic infection. *J Matern Fetal Neonatal Med.* 2005; 17:365–373. [PubMed: 16009638]
153. Tomblom SA, Klimaviciute A, Bystrom B, Chromek M, Brauner A, Ekman-Ordeberg G. Non-infected preterm parturition is related to increased concentrations of IL-6, IL-8 and MCP-1 in human cervix. *Reprod Biol Endocrinol.* 2005; 3:1–10. [PubMed: 15642115]

154. Shynlova O, Tsui P, Dorogin A, Lye SJ. Monocyte chemoattractant protein-1 (CCL-2) integrates mechanical and endocrine signals that mediate term and preterm labor. *J Immunol.* 2008; 181:1470–1479. [PubMed: 18606702]
155. Romero R, Grivel JC, Tarca AL, Chaemsaithong P, Xu Z, Fitzgerald W, Hassan SS, Chaiworapongsa T, Margolis L. Evidence of perturbations of the cytokine network in preterm labor. *Am J Obstet Gynecol.* 2015
156. Lappas M, Permezel M, Georgiou HM, Rice GE. Regulation of proinflammatory cytokines in human gestational tissues by peroxisome proliferator-activated receptor-gamma: effect of 15-deoxy-Delta(12,14)-PGJ(2) and troglitazone. *J Clin Endocrinol Metab.* 2002; 87:4667–4672. [PubMed: 12364456]
157. Meier CA, Chicheportiche R, Juge-Aubry CE, Dreyer MG, Dayer JM. Regulation of the interleukin-1 receptor antagonist in THP-1 cells by ligands of the peroxisome proliferator-activated receptor gamma. *Cytokine.* 2002; 18:320–328. [PubMed: 12160520]

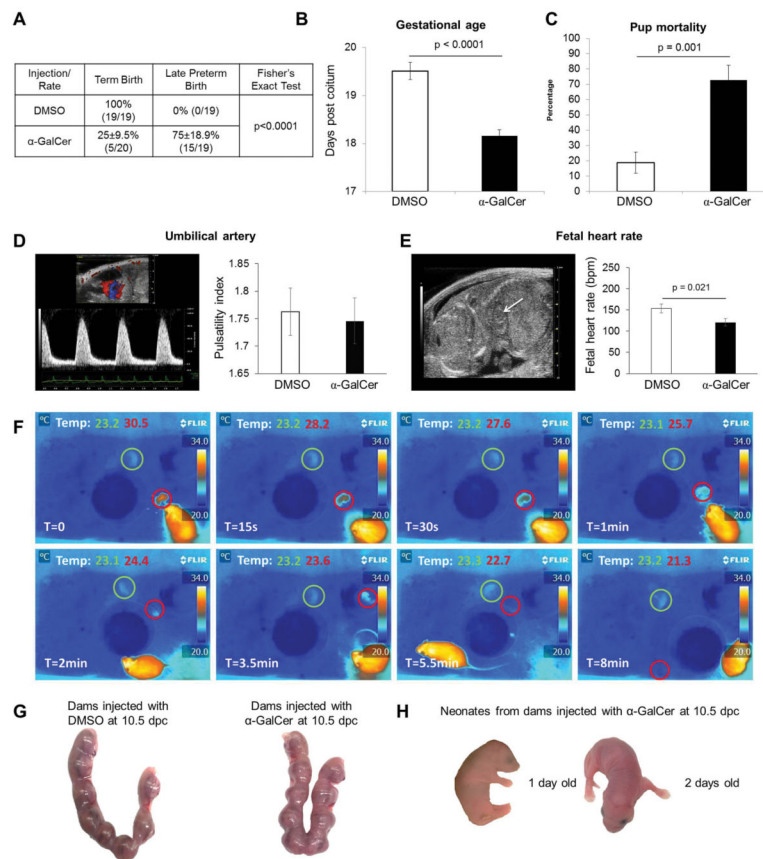


### Figure 1. $\alpha$ -GalCer induces late preterm birth but not pregnancy loss

(A) The rate of term birth was defined as the percentage of dams delivering at  $19.5\pm 0.5$  dpc among all births. The rate of late PTB was defined as the percentage of dams delivering between 18.0 and 18.5 dpc among all births. Data are represented as percentages  $\pm$  95% confidence interval. (B) Gestational age was calculated from the presence of the vaginal plug (0.5 dpc) until the observation of the first pup in the cage bedding. (C) The rate of pup mortality for each litter was defined as the proportion of born pups found dead out of the total litter size. Data (A–C) are from individual dams, n=19–20 each. (D&E) Doppler ultrasound was performed on fetuses just prior to  $\alpha$ -GalCer-induced late PTB in dams injected with  $\alpha$ -GalCer and in time-matched DMSO controls. Umbilical artery pulsatility index and fetal heart rate were recorded. Data are from 3 independent litters. (F) Immediately after  $\alpha$ -GalCer-induced late PTB, the body temperature of the newborns was monitored using a thermal infrared camera. Temperature readings were recorded at intervals of 0, 15, and 30 s, and at intervals of 1, 2, 3.5, 5.5, and 8 min. Data are representative of individual dams, n=3. (G) Uterine horns at 14.5 dpc from dams i.v. injected with DMSO or  $\alpha$ -GalCer on 10.5 dpc. Data are representative of individual dams, n=5 each. (H) Term neonates at 1 day and 2 days old delivered from dams i.v. injected with  $\alpha$ -GalCer on 10.5 dpc. Data are representative of individual dams, n=3.

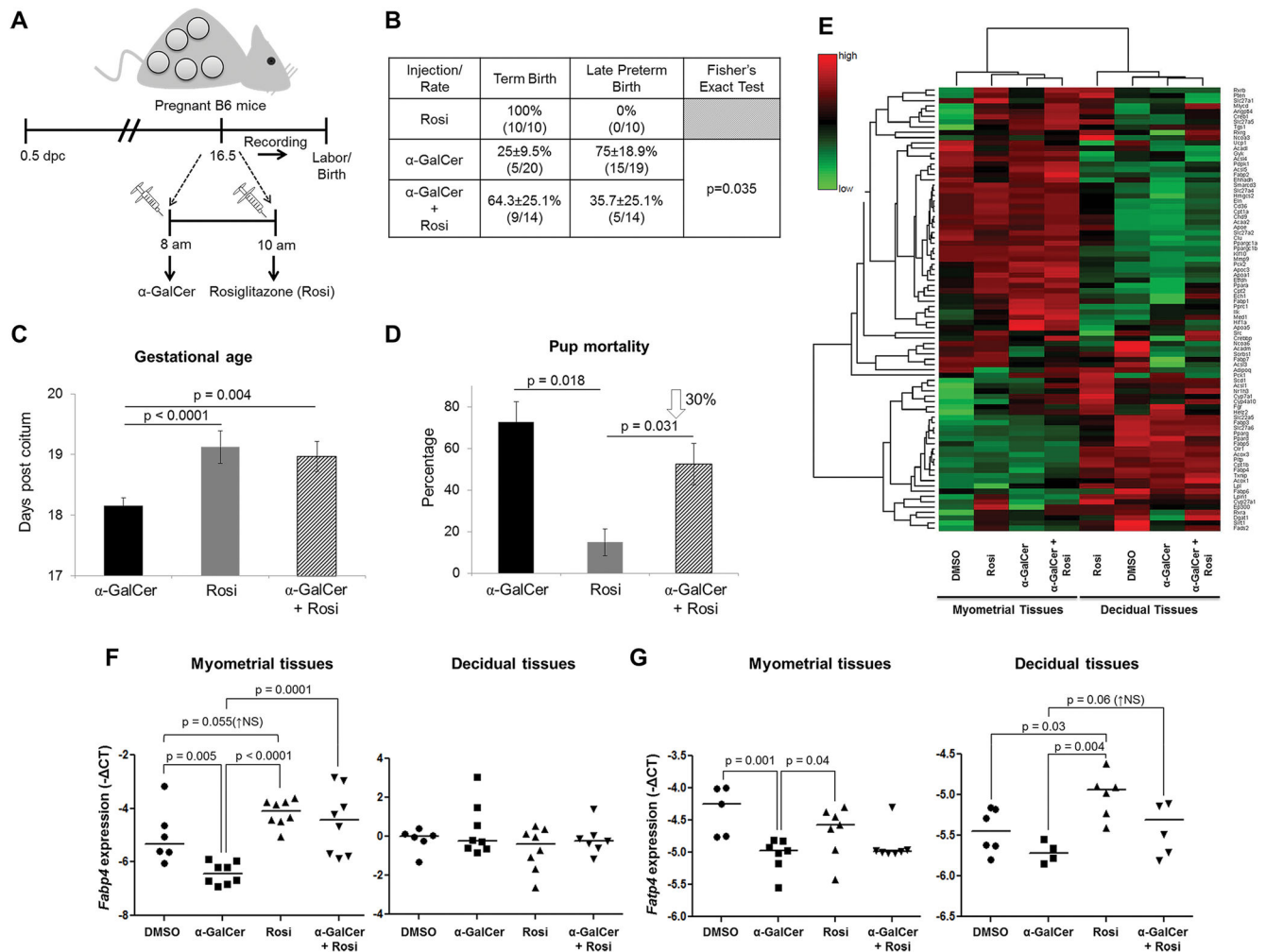


**Figure 2. Rosiglitazone treatment reduces the rate of  $\alpha$ -GalCer-induced late PTB by inducing PPAR $\gamma$  activation at the maternal-fetal interface**

(A) On 16.5 dpc, pregnant mice were i.v. injected with  $\alpha$ -GalCer and treated shortly after with rosiglitazone (Rosi; s.c.) and video monitored (n=14). Control mice were s.c. injected with rosiglitazone alone (n=10). (B) The rate of term birth was defined as the percentage of dams delivering at 19.5 $\pm$ 0.5 dpc among all births. The rate of late PTB was defined as the percentage of dams delivering between 18.0 and 18.5 dpc among all births. Data are represented as percentages  $\pm$  95% confidence interval. (C) Gestational age was calculated from the presence of the vaginal plug (0.5 dpc) until the observation of the first pup in the cage bedding. (D) The rate of pup mortality for each litter was defined as the proportion of born pups found dead out of the total litter size. (E) A heat map visualization of PPAR targets gene expression in myometrial and decidual tissues from dams i.v. injected with DMSO,  $\alpha$ -GalCer, rosiglitazone, or  $\alpha$ -GalCer + rosiglitazone. Data are from individual dams, n=4 each. (F) mRNA expression of *Fabp4* in myometrial and decidual tissues. (G) mRNA expression of *Fatp4* in myometrial and decidual tissues. Negative CT values (F&G) were calculated using *Actb* as a reference gene. Data are from individual dams, n=6–8 each.

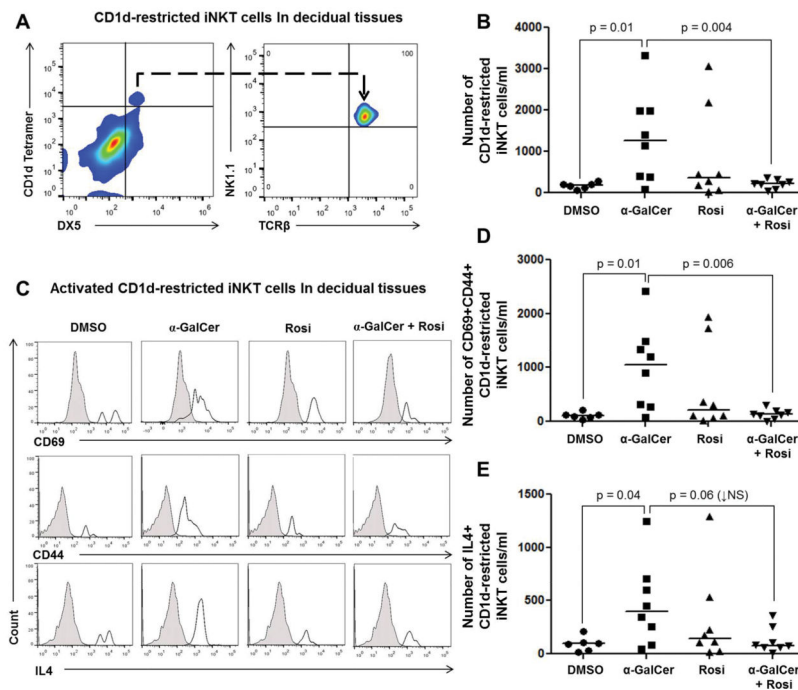


**Figure 3. Administration of  $\alpha$ -GalCer induces an expansion of activated CD1d-restricted iNKT cells in decidual tissues, which is blunted by rosiglitazone**

(A) Gating strategy used to identify CD1d-restricted iNKT cells (CD1d tetramer +DX5+NK1.1+TCR $\beta$ + cells) in decidual tissues. (B) Number of CD1d-restricted iNKT cells in decidual tissues from mice injected with DMSO,  $\alpha$ -GalCer, rosiglitazone, or  $\alpha$ -GalCer + rosiglitazone. Data are from individual dams, n=6–8 each. (C) Immunophenotyping of activation markers CD69, CD44, and IL4 in CD1d-restricted iNKT cells in decidual tissues from mice injected with DMSO,  $\alpha$ -GalCer, rosiglitazone (Rosi), or  $\alpha$ -GalCer + rosiglitazone. The gray histogram represents the autofluorescence control, and the white histogram represents the fluorescence signal from CD1d-restricted iNKT cells. (D&E) Number of CD69+CD44+ or IL4+CD1d-restricted iNKT cells in decidual tissues from mice injected with DMSO,  $\alpha$ -GalCer, rosiglitazone, or  $\alpha$ -GalCer + rosiglitazone. Data are from individual dams, n=6–8 each.

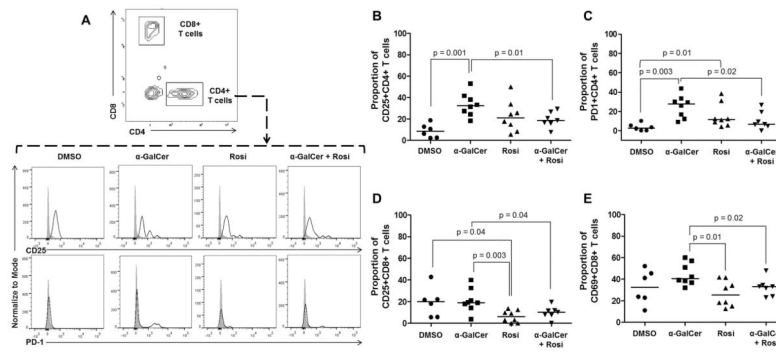


**Figure 4. Administration of  $\alpha$ -GalCer induces activation of CD4+ T cells in myometrial tissues that is reduced by rosiglitazone**

(A) Gating strategy used to identify activated CD4+ T cells (CD3+CD4+ cells) in myometrial tissues. Immunophenotyping of activation markers CD25 and PD1 in CD4+ T cells in myometrial tissues from mice injected with DMSO,  $\alpha$ -GalCer, rosiglitazone (Rosi), or  $\alpha$ -GalCer + rosiglitazone. The gray histogram represents the autofluorescence control, and the white histogram represents the fluorescence signal from CD4+ T cells. (B&C) Proportion of CD25+CD4+ T cells and PD1+CD4+ T cells in myometrial tissues from mice injected with DMSO,  $\alpha$ -GalCer, rosiglitazone, or  $\alpha$ -GalCer + rosiglitazone. Data are from individual dams, n=6–8 each. (D&E) Proportion of CD25+CD8+ T cells and CD69+CD8+ T cells in myometrial tissues from mice injected with DMSO,  $\alpha$ -GalCer, rosiglitazone, or  $\alpha$ -GalCer + rosiglitazone. Data are from individual dams, n=6–8 each.

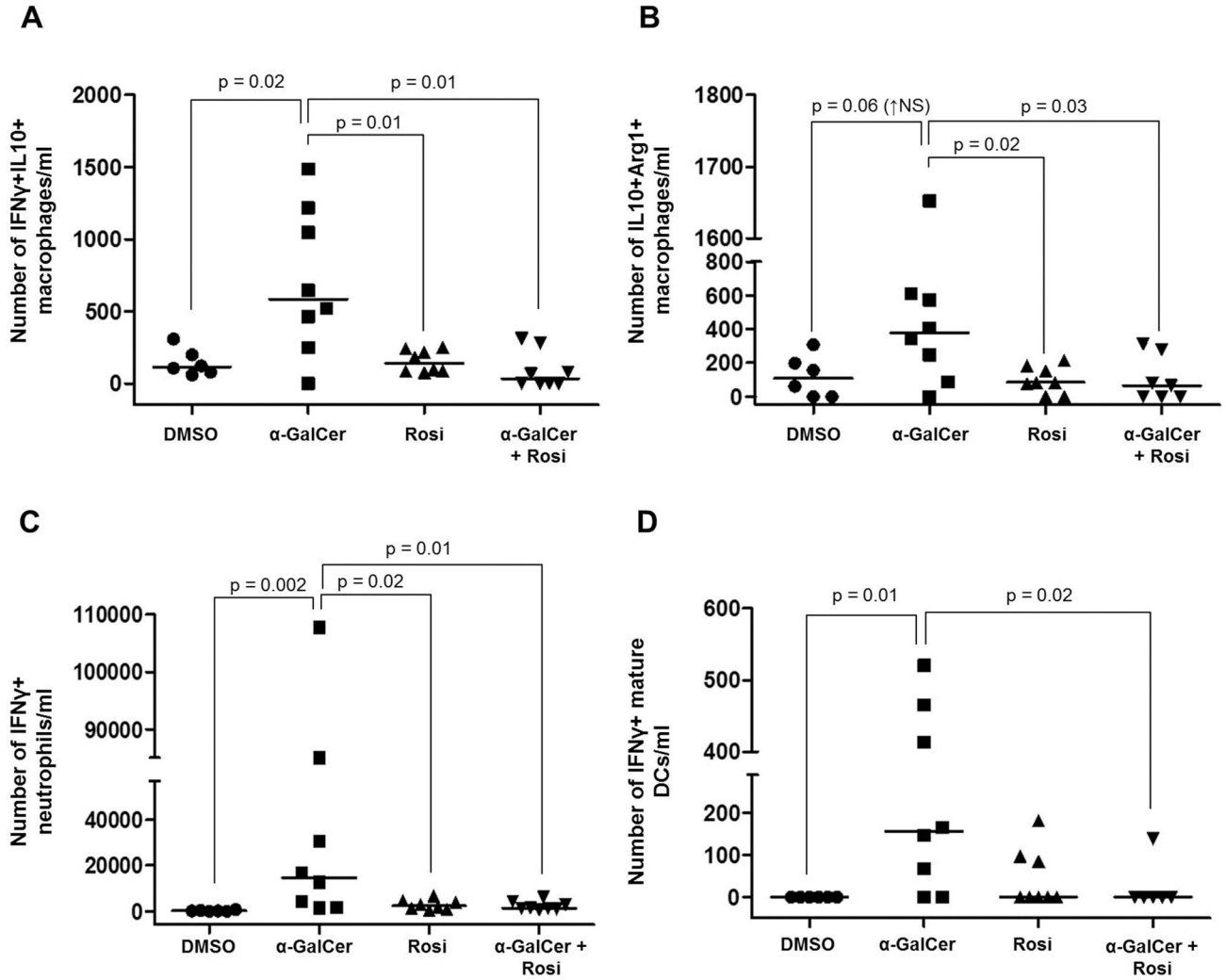


**Figure 5. Administration of  $\alpha$ -GalCer induces activation of innate immune cells at the maternal-fetal interface that is blunted by rosiglitazone**

(A) Number of activated IFN $\gamma$ +IL10+ macrophages in decidual tissues from mice injected with DMSO,  $\alpha$ -GalCer, rosiglitazone, or  $\alpha$ -GalCer + rosiglitazone. Data are from individual dams, n=6–8 each. (B) Number of activated IL10+Arg1+ macrophages in decidual tissues from mice injected with DMSO,  $\alpha$ -GalCer, rosiglitazone, or  $\alpha$ -GalCer + rosiglitazone. Data are from individual dams, n=6–8 each. (C) Number of activated IFN $\gamma$ + neutrophils in decidual tissues from mice injected with DMSO,  $\alpha$ -GalCer, rosiglitazone, or  $\alpha$ -GalCer + rosiglitazone. Data are from individual dams, n=6–8 each. (D) Number of IFN $\gamma$ + mature DCs in decidual tissue from mice injected with DMSO,  $\alpha$ -GalCer, rosiglitazone, or  $\alpha$ -GalCer + rosiglitazone. Data are from individual dams, n=6–8 each.



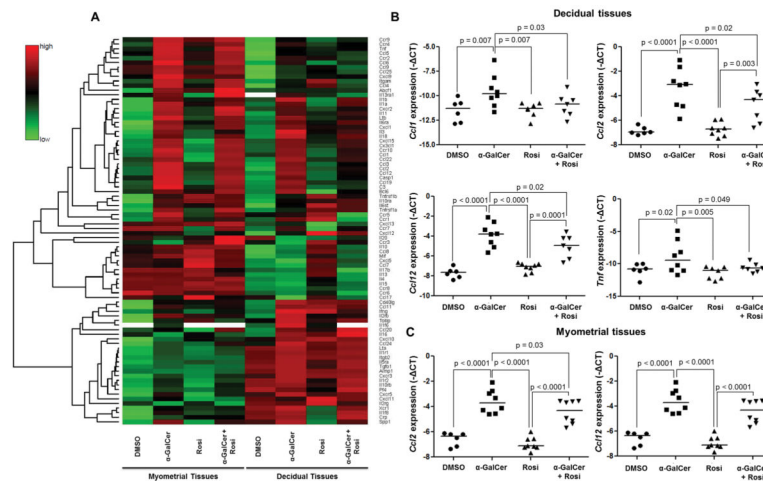


**Figure 6. Administration of  $\alpha$ -GalCer induces a pro-inflammatory microenvironment at the maternal-fetal interface that is partially attenuated by rosiglitazone**  
**(A)** A heat map visualization of cytokine and chemokine gene expression in myometrial and decidual tissues from dams i.v. injected with DMSO,  $\alpha$ -GalCer, rosiglitazone (Rosi) or  $\alpha$ -GalCer + rosiglitazone. Data are from individual dams, n=4 each. **(B)** mRNA expression of *Ccl1*, *Ccl2*, *Ccl12*, and *Tnf* in decidual tissues. Negative  $\Delta$  Ct values were calculated using *Actb* as a reference gene. Data are from individual dams, n=6–8 each. **(C)** mRNA expression of *Ccl2* and *Ccl12* in myometrial tissues. Negative  $\Delta$  Ct values (B&C) were calculated using *Actb* as a reference gene. Data are from individual dams, n=6–8 each.

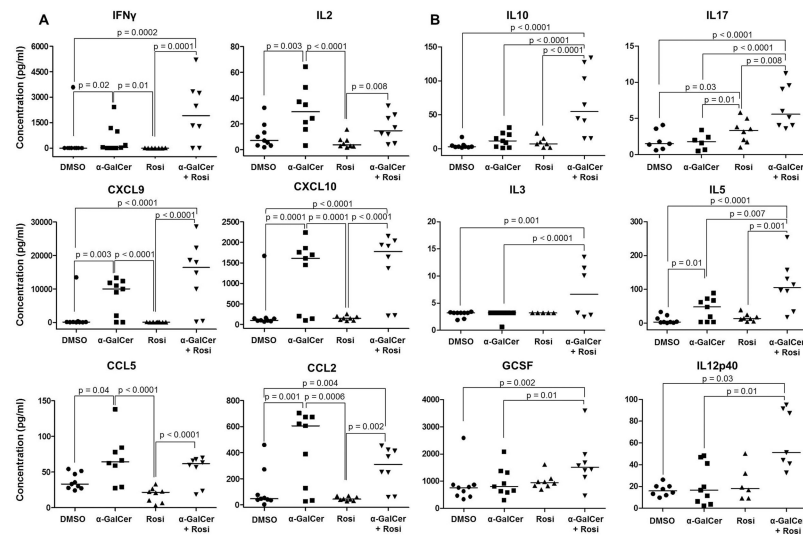


**Figure 7. Administration of  $\alpha$ -GalCer induces a maternal systemic pro-inflammatory response yet rosiglitazone drives a maternal systemic anti-inflammatory response**  
 Pregnant mice were i.v. injected with DMSO,  $\alpha$ -GalCer, rosiglitazone (Rosi), or  $\alpha$ -GalCer + rosiglitazone. Serum concentrations of pro-inflammatory (**A**) and anti-inflammatory (**B**) cytokines/chemokines were determined 24 h after the initial injection. Data are from individual dams, n=8–9 each.

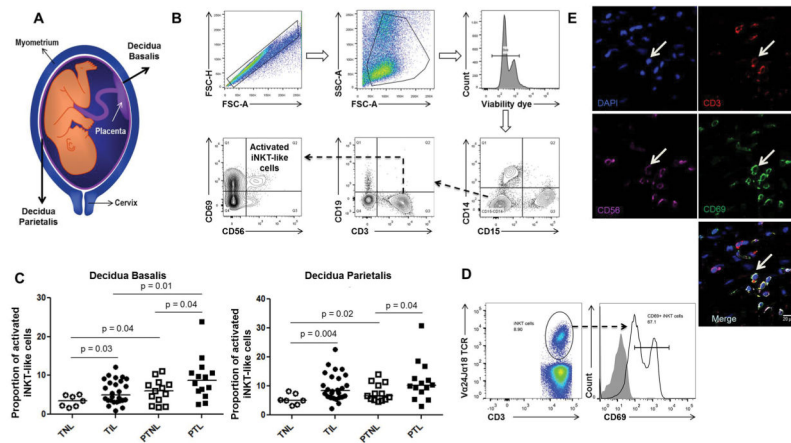


**Figure 8. Spontaneous preterm labor/birth is associated with an increased proportion of activated iNKT-like cells in decidual tissues**

(A) Schematic representation to localize the decidua basalis and decidua parietalis. (B) Gating strategy used to identify activated iNKT-like cells (CD69+CD56+CD3+CD19-CD14-CD15- cells) in human decidual tissue. (C) Activated i-iNKT-like cells in the decidua basalis or decidua parietalis from women who underwent spontaneous term labor (TIL) or spontaneous preterm labor (PTL). Controls included samples from women who delivered at term (TNL) or preterm (PTNL) without labor. Data are from individual women: n=7 for TNL, n=27 for TIL, n=13 for PTNL, and n=14 for PTL. (D) Identification of CD3+V $\alpha$ 24J $\alpha$ 18TCR+CD69+ cells in PTL decidual tissues. (E) Identification of activated iNKT-like cells in the decidua parietalis by confocal microscopy. Nuclei are blue (DAPI), CD3+ cells are red (Alexa Fluor 594), CD56+ cells are magenta (APC), and CD69+ cells are green (FITC). White arrows represent activated NKT cells. Scale bars: 20  $\mu$ m.

**Table 1**

Demographic and clinical characteristics of the study populations

Demographic or clinical characteristic	TNL (n=7)	TIL (n=26)	PTNL (n=13)	PTL (n=14)	P value
Maternal age (years)*	28 (23–32)	23.5 (22–27)	25 (22–30)	22 (19.5–25)	NS
Race**					
African-American	7 (100%)	26 (100%)	11 (84.6%)	13 (92.9%)	
Caucasian	0 (0.0%)	0 (0.0%)	1 (7.7%)	1 (7.1%)	NS
Hispanic	0 (0.0%)	0 (0.0%)	0 (0.0%)	0 (0.0%)	
Other	0 (0.0%)	0 (0.0%)	1 (7.7%)	0 (0.0%)	
Maternal weight (kg)*	93 (68.8–98.7)	90.05 (71.1–106.0)	74.8 (62.6–102.7)	75.6 (56.7–88.2)	NS
Body mass index (kg/m <sup>2</sup> )*	31.2 (26.35–41.45)	33.9 (27.38–39.25)	32.8 (23–39.4)	28.35 (21.53–31.6)	NS
Primiparity**	0 (0%)	6 (23.08%)	3 (23.08%)	1 (7.14%)	NS
Gestational age at delivery (weeks)*	39 (38.5–39.5)	39.4 (38.2–39.9)	34.9 (32–36.1)	34.2 (31.2–35.3)	<0.0001
Birth weight (grams)*	3005 (2855–3073)	3240 (2906–3419)	1510 (1255–2375)	2148 (1674–2554)	<0.0001
Cesarean section**	100%	15.4%	100%	14.3%	<0.0001
Chronic chorioamnionitis**	28.6%	30.8%	46.2%	21.4%	NS
Acute chorioamnionitis**	0%	34.6%	7.7%	42.8%	NS
Smoked during Pregnancy**					
Yes	1 (14.3%)	5 (19.2%)	2 (15.4%)	0 (0%)	NS
No	6 (85.7%)	21 (80.8%)	11 (84.6%)	14 (100%)	

\* Kruskal-Wallis test

\*\* Chi-square test